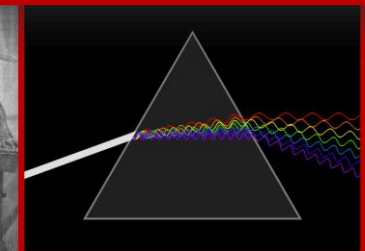


SPECTROSCOPIC STUDY OF CO IN THE FUNDAMENTAL BAND OVER A RANGE OF TEMPERATURES FROM 296 TO 79 K

Adriana Predoi-Cross

with contributions from enthusiastic graduate
students at University of Lethbridge and research
collaborators from Canada and abroad

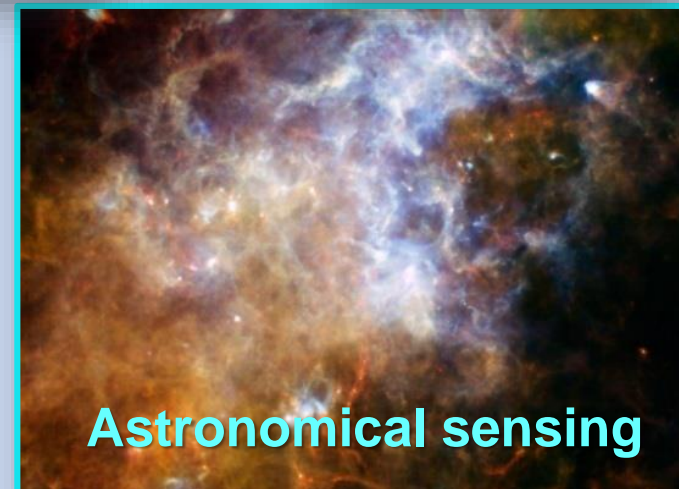
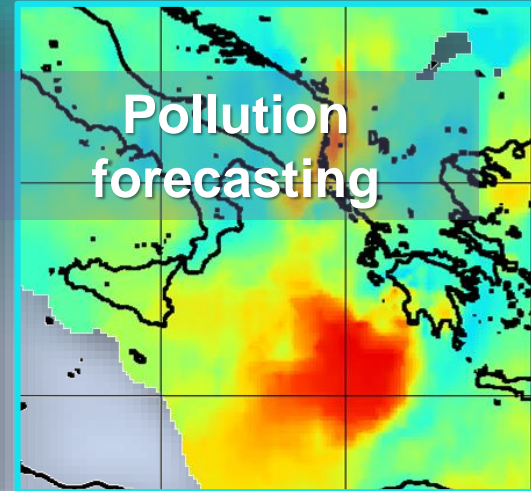
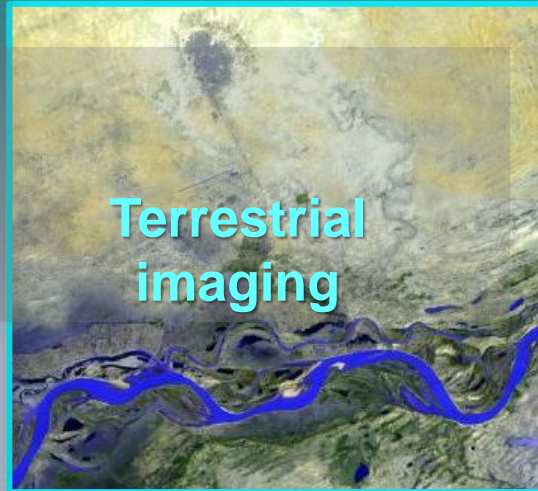
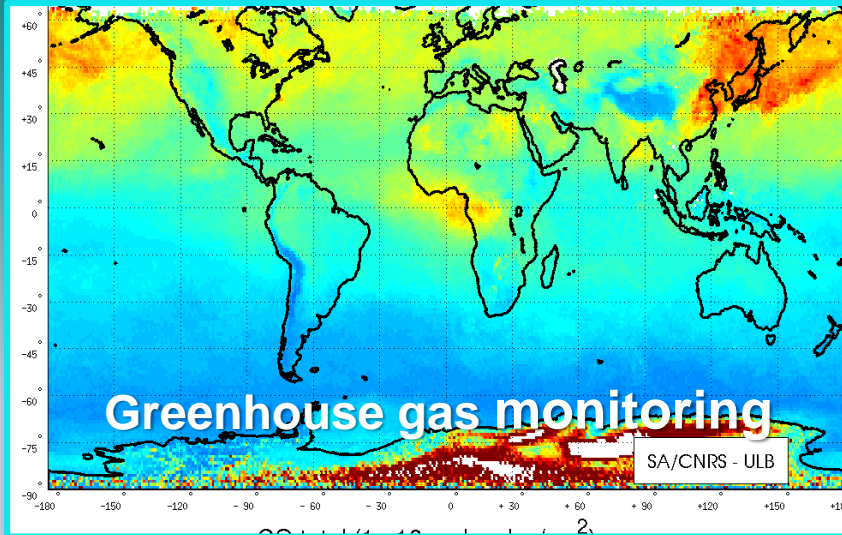


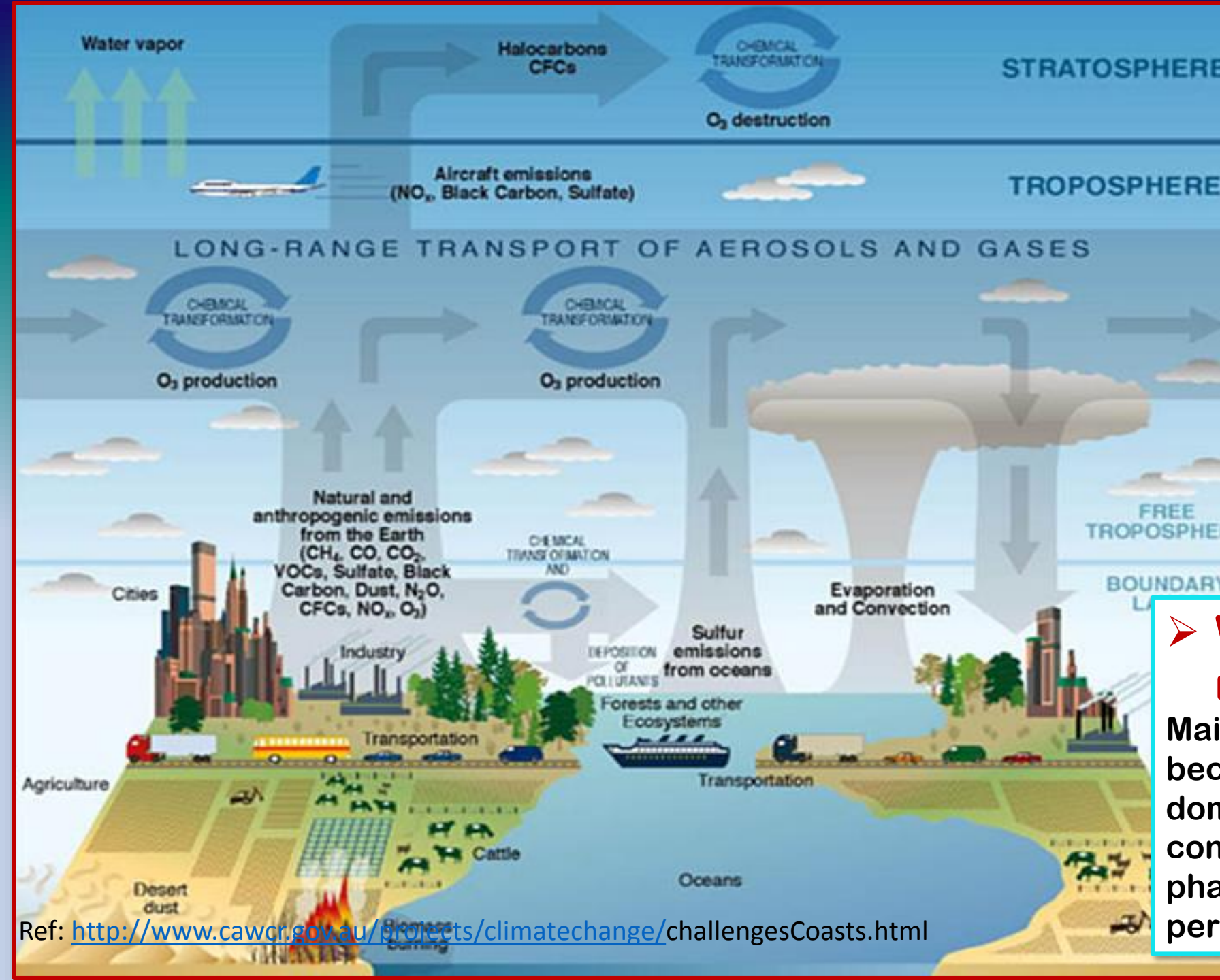
OUTLINE OF MY PRESENTATION

- **Research Context**
- **Theoretical Explorations**
- **Fourier transform spectroscopic studies of carbon monoxide broadened by CO, air, He in the fundamental band**
- **Conclusion and Directions for Future Work**
- **References**
- **Funding sources**

Research Context

Combining the results of laboratory studies and from theoretical models with results from remote sensing measurements, it is possible to determine the chemical composition and physical properties of the remote environments. This is the basis of **spectroscopic remote sensing**, a technique that is widely used in planetary atmospheric exploration.





Questions:

- How much of the change that we observe in the Earth's atmosphere is due to human activities?
- Do we understand the system Earth well enough to predict and quantify the impact of human activities?

➤ What do we need to measure?

Mainly gases and aerosols because atmospheric chemistry is dominated by reactions of trace constituents, specifically gas phase radicals, present in parts per million, billion, trillion.

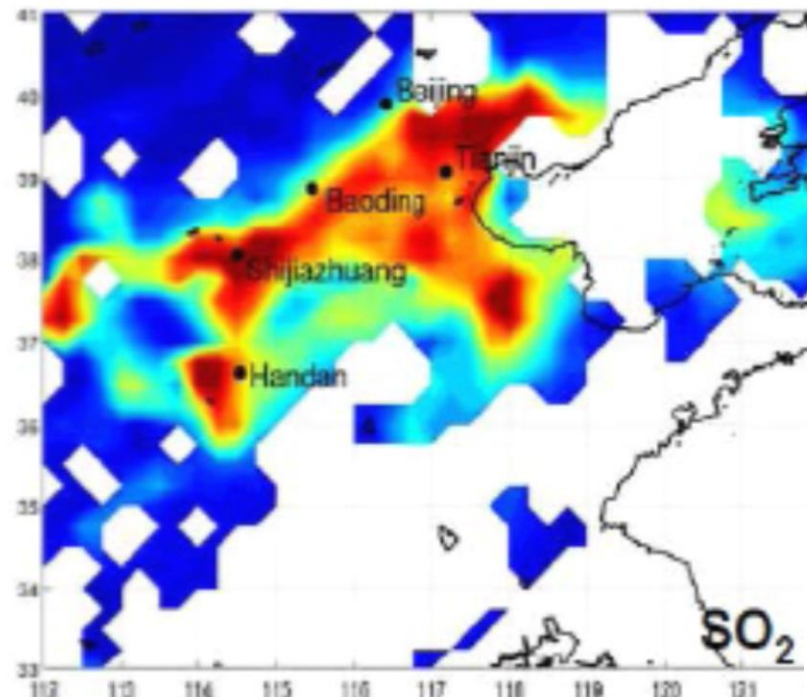
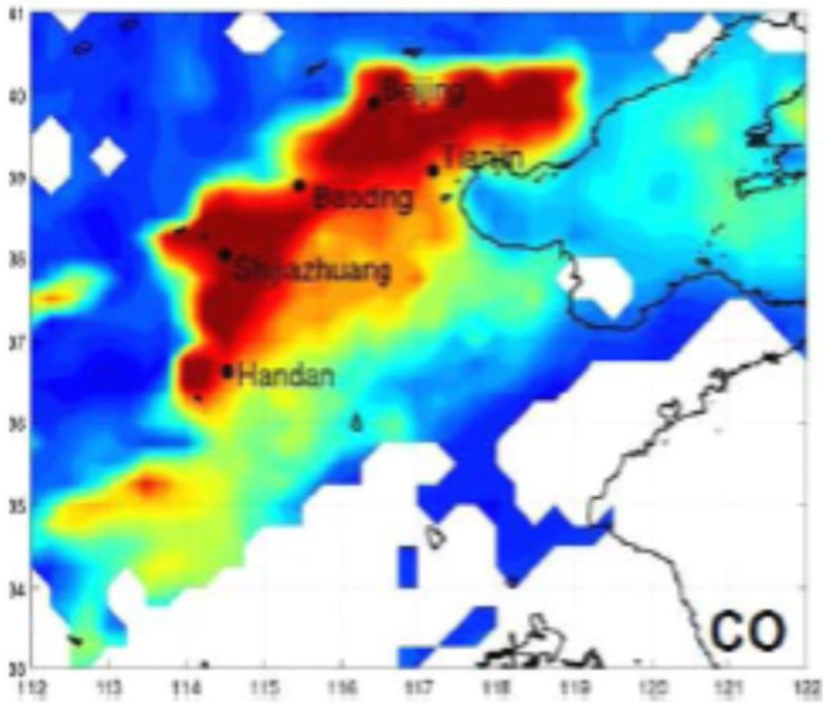
Case example: Air pollution studies

The Guardian: According to an official monitoring centre in Beijing, levels of PM2.5 were well above 600 micrograms per cubic metre in several places on Saturday, and may even have hit 900. Though Monday's level dropped to around 350, that is still far above the safe level of 25 designated by the World Health Organisation.

What we see



What spectrometers (hyperspectral) see



**Spectroscopy
reveals
atmospheric
composition**

Courtesy of Dr. Pierre Coheur,
Spectroscopie de l'Atmosphère,
Université Libre de Bruxelles, Belgium

Analysis details for Fourier transform spectra recorded at different sets of pressure, temperatures and pathlength

- The wavenumber scales were calibrated using line positions in the HITRAN2012 database.
- The interactive multispectrum nonlinear least squares **fitting technique** (Benner *et al.* (1995)) was used to analyze **all spectra recorded, simultaneously**. It uses the **Levenberg-Marquardt algorithm** that minimizes the sum of the squares of the **residuals** between the **experimental spectra** and the spectra **calculated** using the fixed and fitted parameters [6].
- **Different line shape profiles were applied such as Voigt or Rautian**. Including **speed-dependence** in our spectral profiles did improve the fit residuals (observed-calculated). **Weak line mixing** was necessary to accurately model the absorption.
- **Initial values** for all line parameters were taken from the HITRAN2012 database.
- **Spectral backgrounds** (including some channeling), zero transmission levels, instrument line shapes were appropriately modeled.

Expressions used in retrievals of broadening and shift parameters

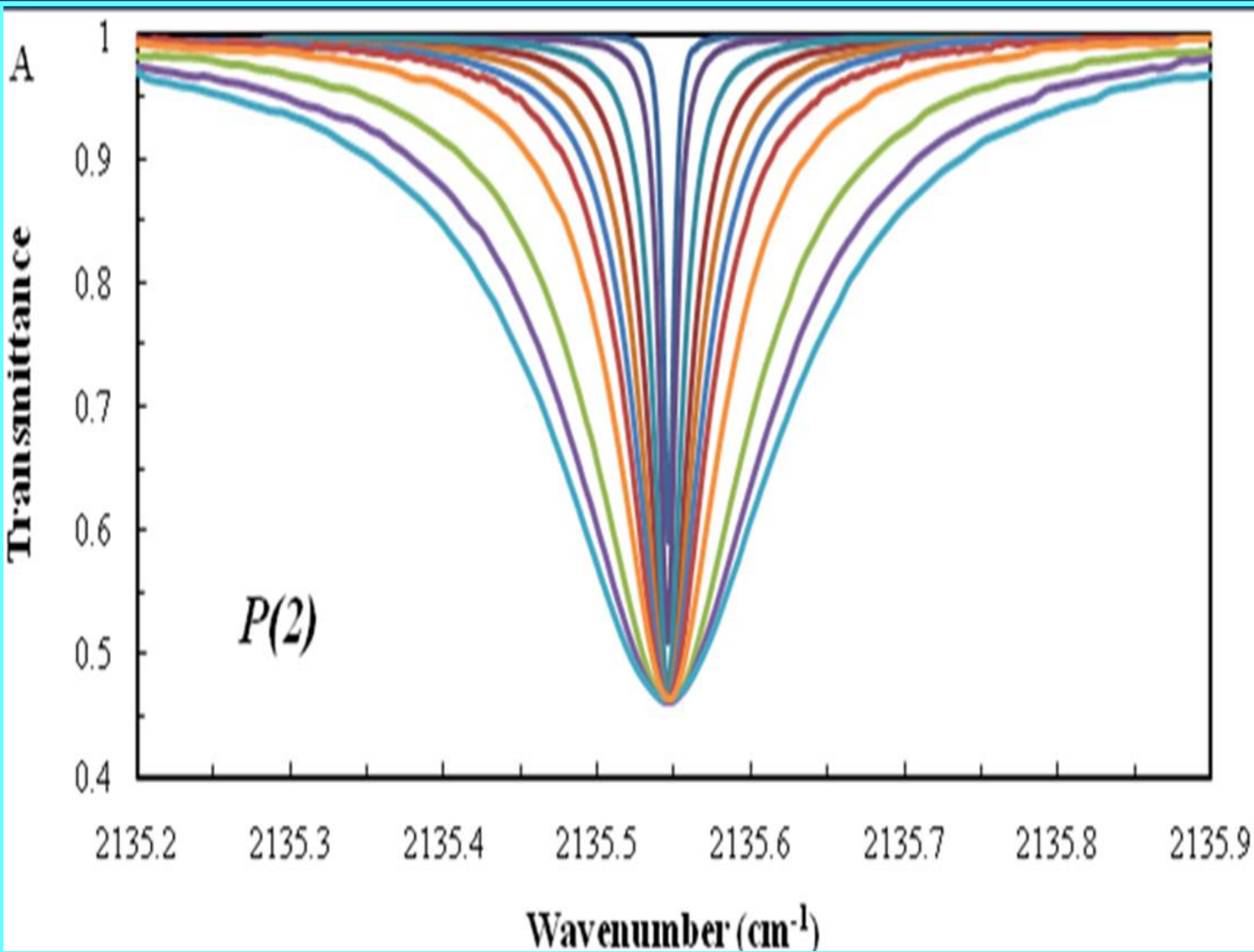
$$b_L(p, T) = p \left[b_L^0(\textit{foreign})(p_0, T_0)(1 - \chi) \left[\frac{T_0}{T} \right]^{n1} + b_L^0(\textit{self})(p_0, T_0) \chi \left[\frac{T_0}{T} \right]^{n2} \right]$$

$b_L(p, T)$ is the Lorentz halfwidth (in cm^{-1}) of the spectral line at pressure p and temperature T , and the broadening coefficient $b_L^0(\textit{Gas})(p_0, T_0)$ is the Lorentz halfwidth of the line at the reference pressure p_0 (1 atm) and temperature T_0 (296 K), and χ is the ratio of the partial pressure of CO to the total sample pressure in the cell. The temperature dependence exponents of the pressure-broadening coefficients are $n1$ and $n2$.

$$\nu = \nu_0 + p \left[\delta^0(\textit{foreign})(1 - \chi) + \delta^0(\textit{self}) \chi \right]$$

where ν_0 is the zero-pressure line position (in cm^{-1}), ν is the line position corresponding to the pressure p , δ^0 is the pressure-induced line shift coefficient at the reference pressure p_0 (1 atm) and temperature T_0 (296 K) of the broadening gas (foreign or self broadener).

Spectral shape of an isolated line



The absorption coefficient is given by

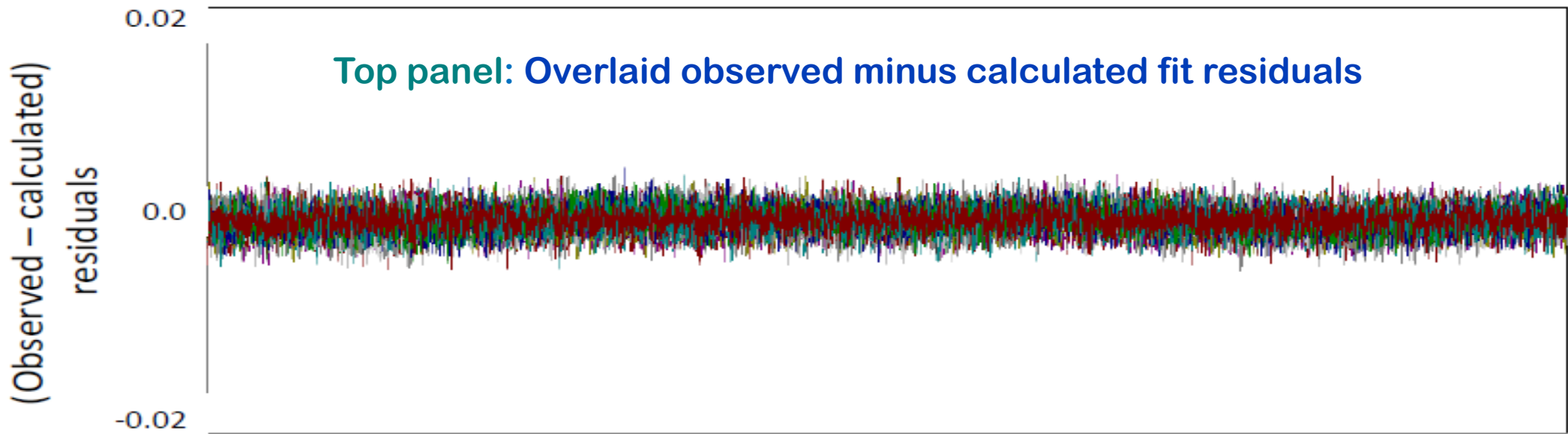
$$\alpha_{fi}(\sigma) = S_{fi} I_{fi}(\sigma - \sigma_{fi})$$

→ Line intensity is distributed around the line position

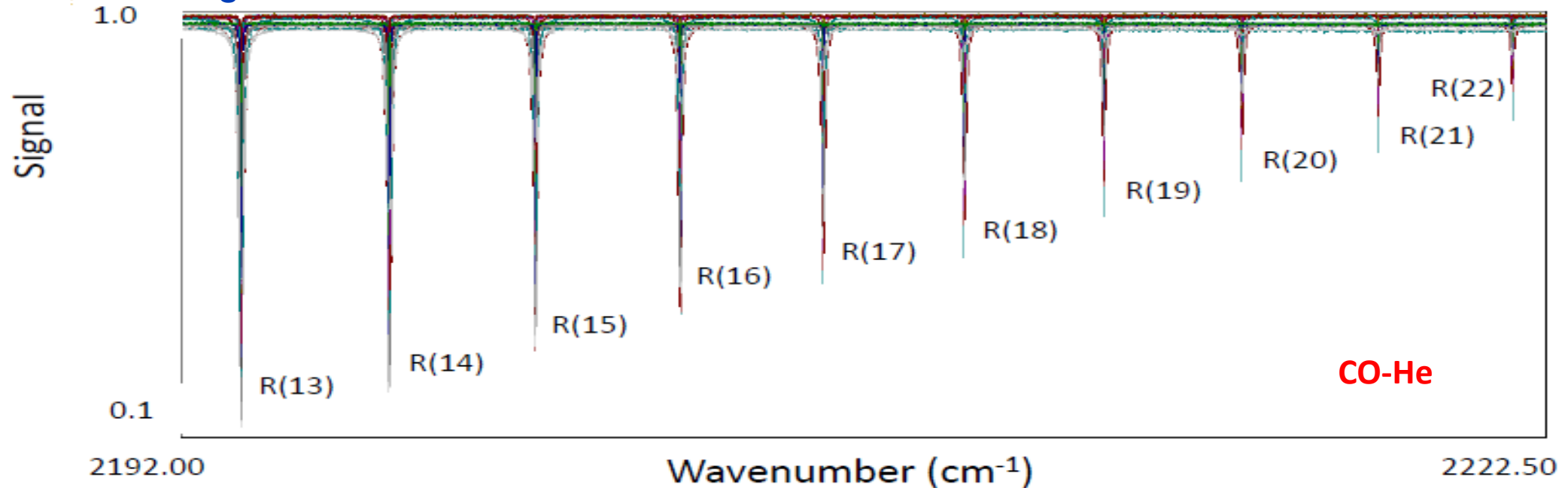
$$S_{fi} = \int_{\sigma_{fi} - \Delta\sigma}^{\sigma_{fi} + \Delta\sigma} d\sigma \alpha_{fi}(\sigma) \cong \int_{-\infty}^{+\infty} d\sigma \alpha_{fi}(\sigma)$$

→ Normalized line profile $I_{fi}(\sigma)$

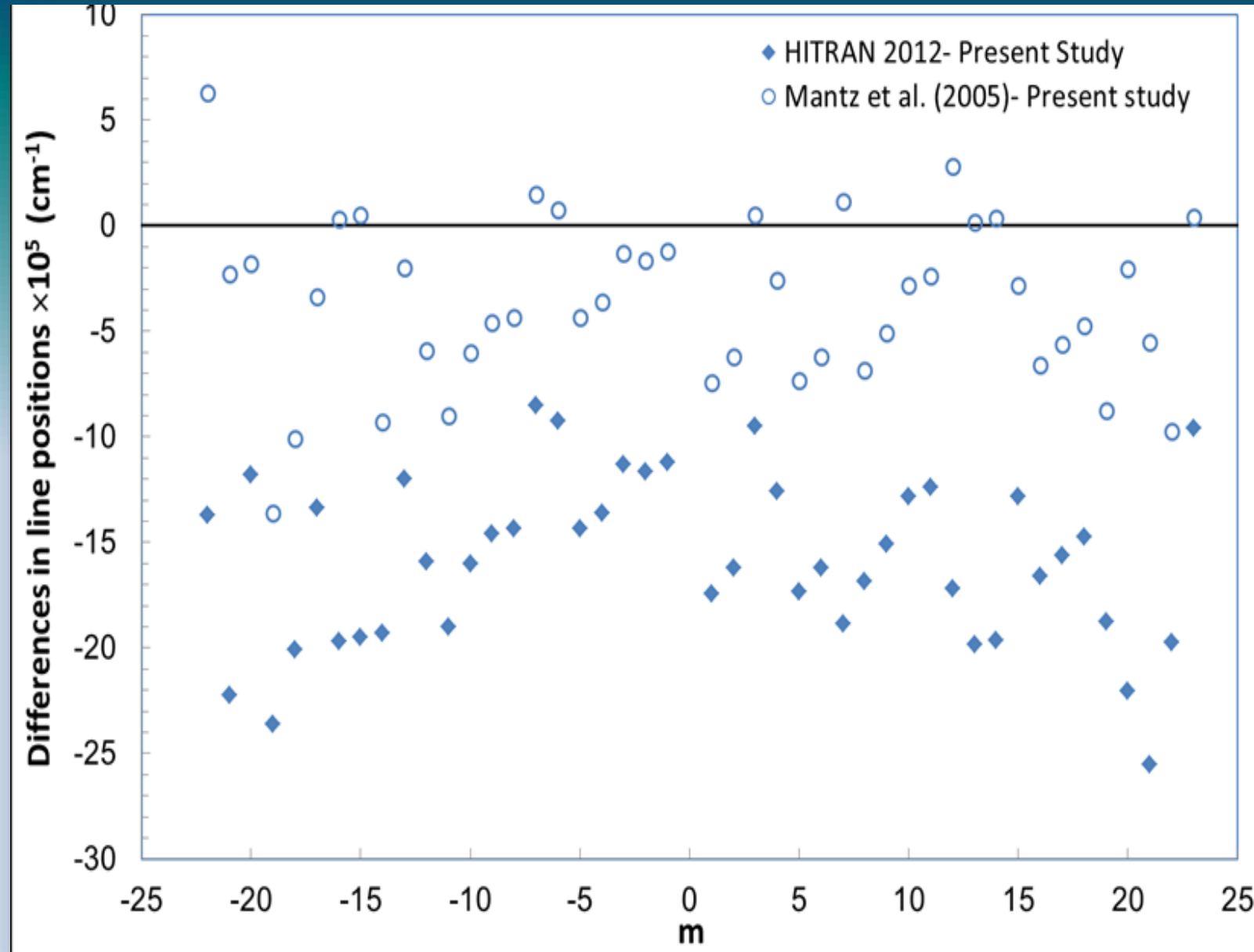
$$\int_{-\Delta\sigma}^{+\Delta\sigma} d\sigma I_{fi}(\sigma) \cong \int_{-\infty}^{+\infty} d\sigma I_{fi}(\sigma) = 1$$



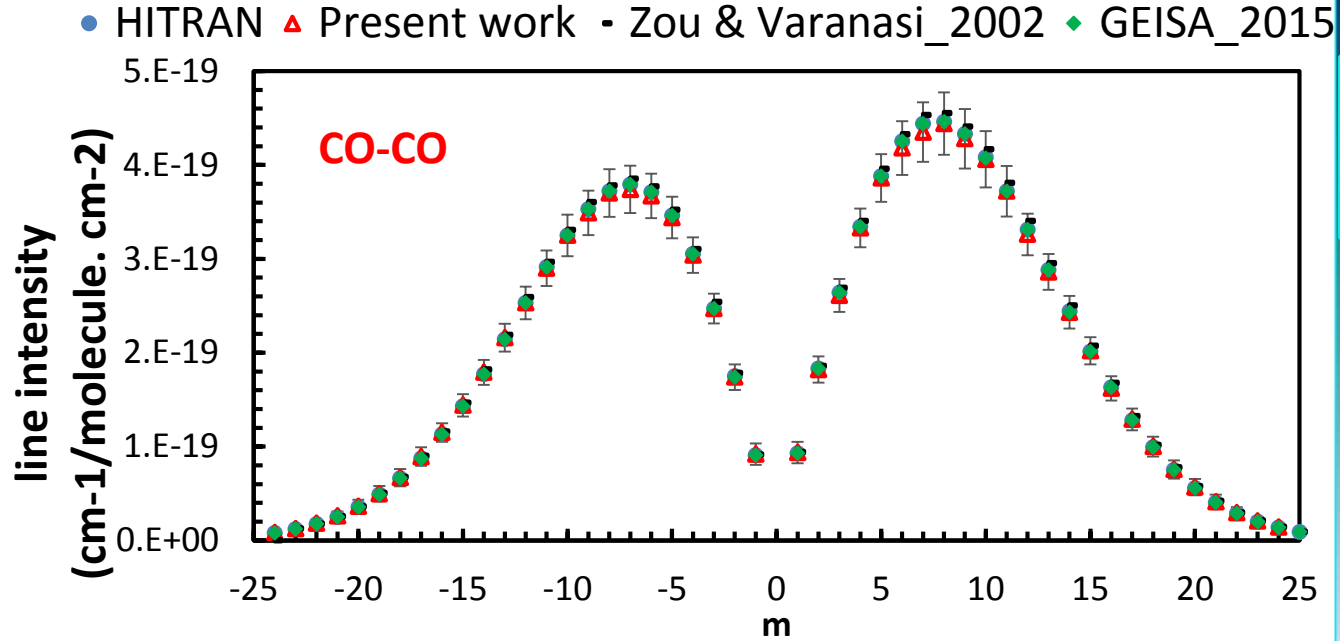
Bottom panel: A section of the 19 overlaid experimental spectra analyzed applying the multispectrum nonlinear least squares fitting technique using the speed dependent Voigt profile with weak line mixing.



Differences between the line positions retrieved in the present study, in HITRAN2012 database and the results of the constrained multispectrum fit analysis reported in Mantz *et al.* J. Mol. Struct. 2005.



Analysis Results for Line Intensities



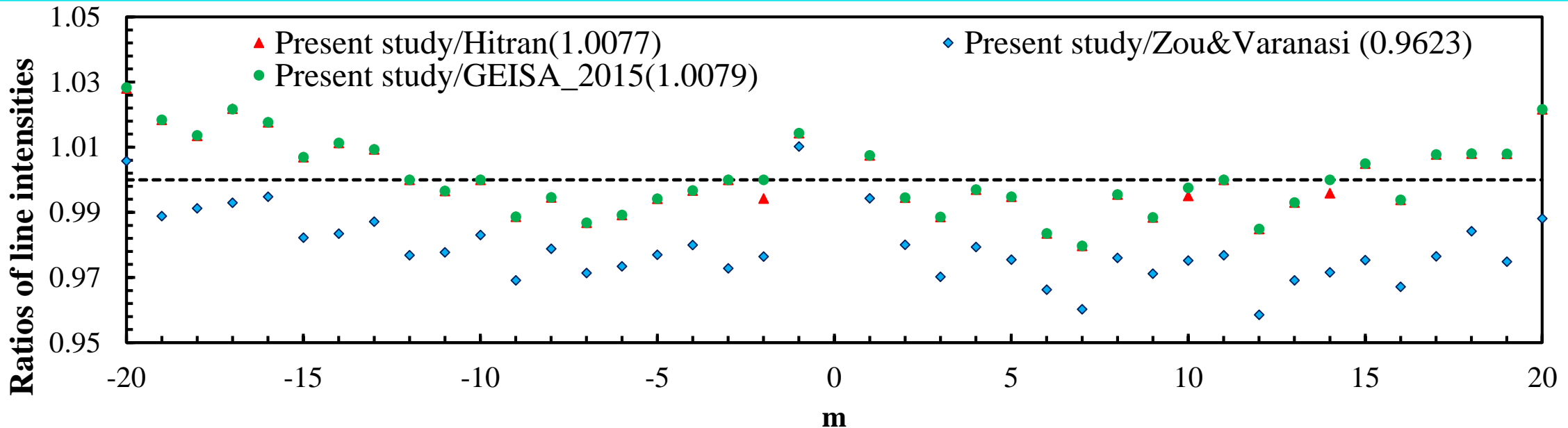
$$S_{ij} = I_a \frac{A_{ij}}{8\pi c \nu_{ij}^2} \frac{g' e^{-c_2 E''/T} (1 - e^{c_2 \nu_{ij}/T})}{Q(T)}$$

$$I_a = 99.998\%$$

$Q(T)$ = Internal partition sum (107.12)

Second radiation constant, $c_2 = hc/k$

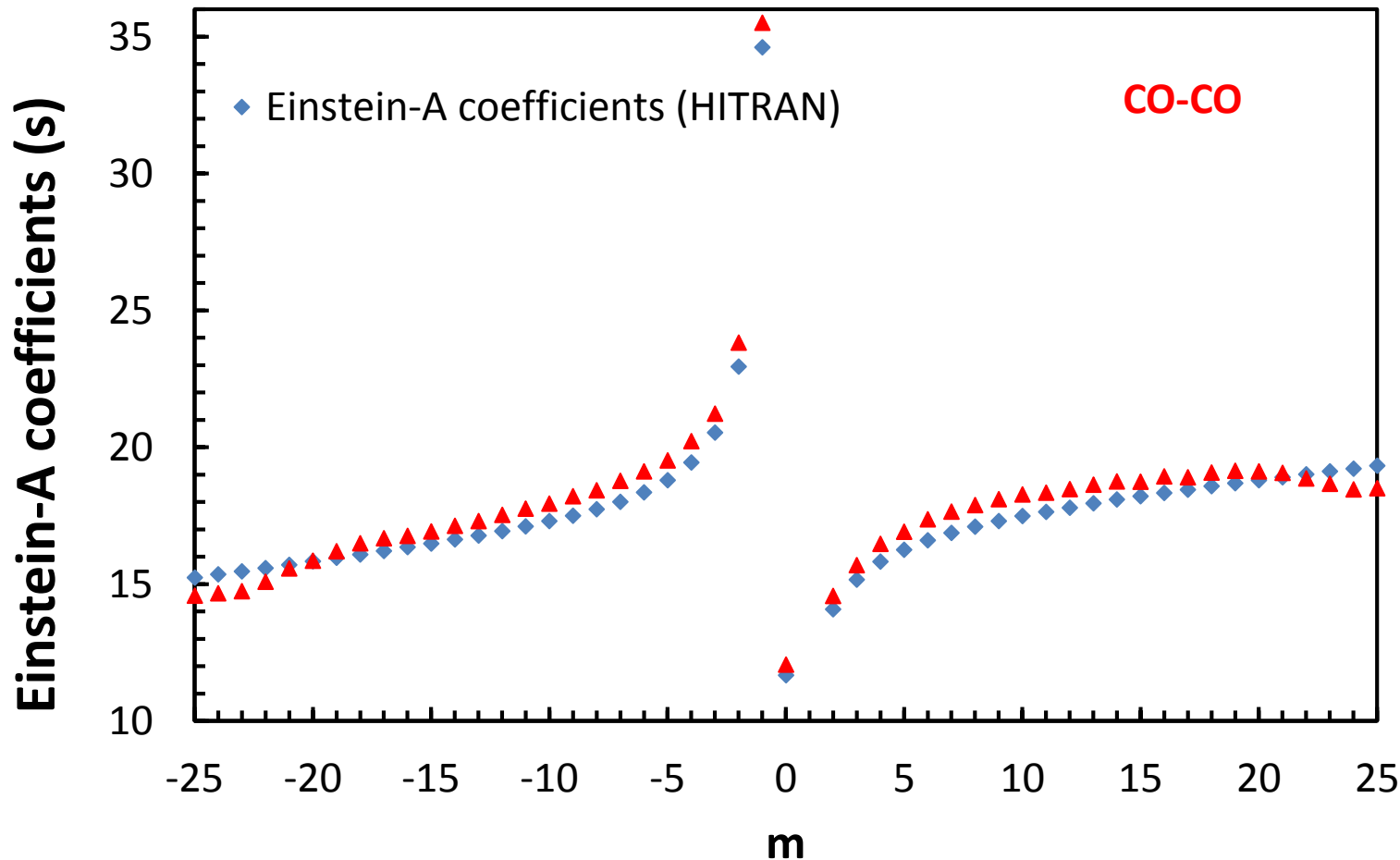
g' = statistic weight at the upper state.



Einstein A coefficients (s⁻¹)

.. define the probability of emission or absorption of light during a molecular transition.

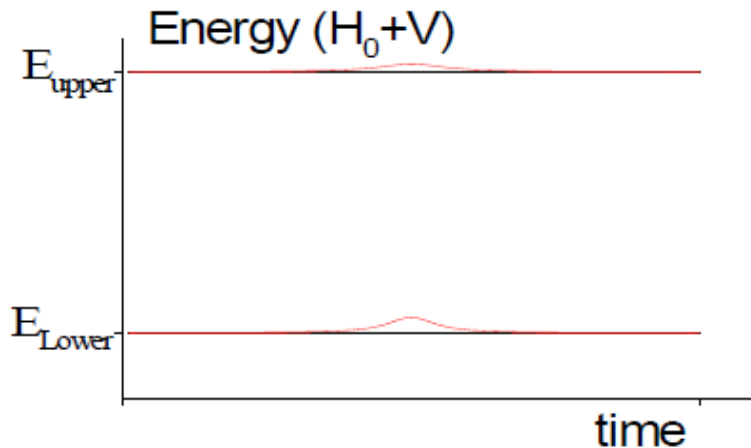
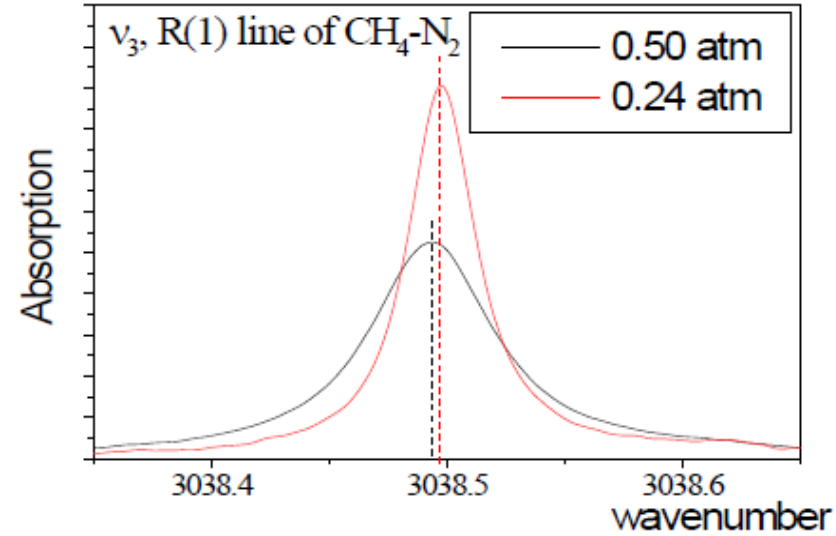
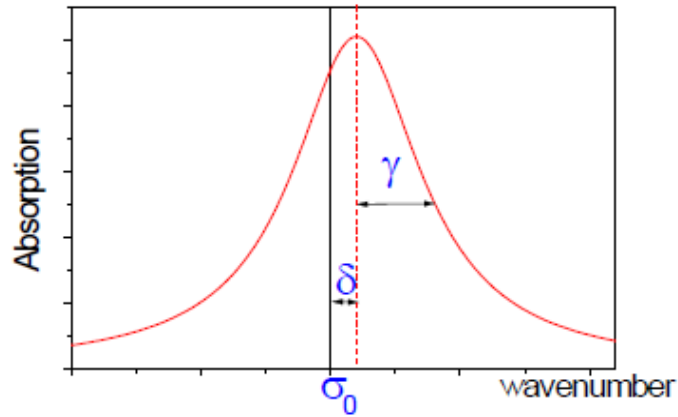
$$S_{ij} = I_a \frac{A_{ij}}{8\pi c \nu_{ij}^2} \frac{g' e^{-c_2 E''/T} (1 - e^{c_2 \nu_{ij}/T})}{Q(T)}$$



$$\frac{S_{ij}(\text{Hitran})}{S_{ij}(\text{PS})} = \frac{A_{ij}(\text{Hitran})}{v_{ij}^2(\text{Hitran})} \cdot \frac{v_{ij}^2(\text{PS})}{A_{ij}(\text{PS})}$$

Line Broadening Effects

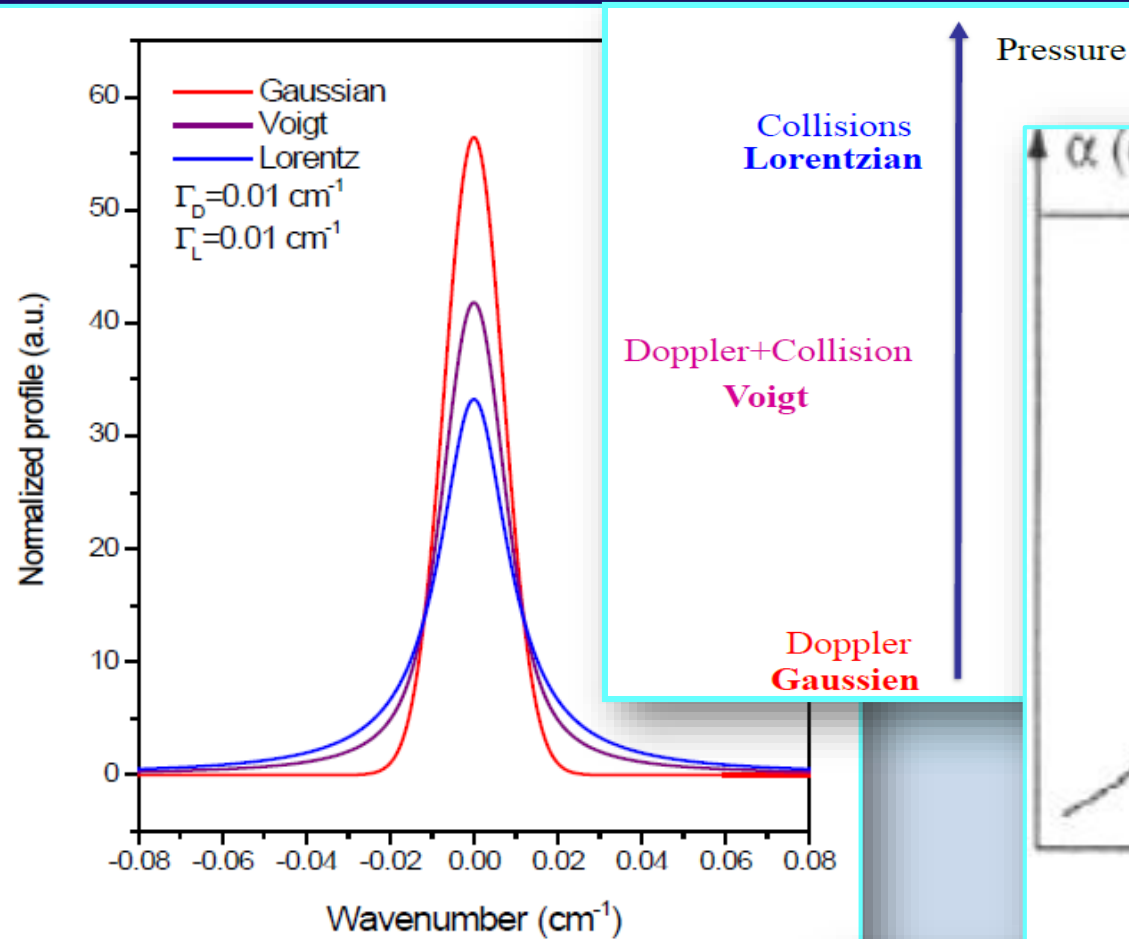
For an isolated transition, the **main** effects of intermolecular collisions (pressure) are the (Lorentz) **broadening and shifting** of the line



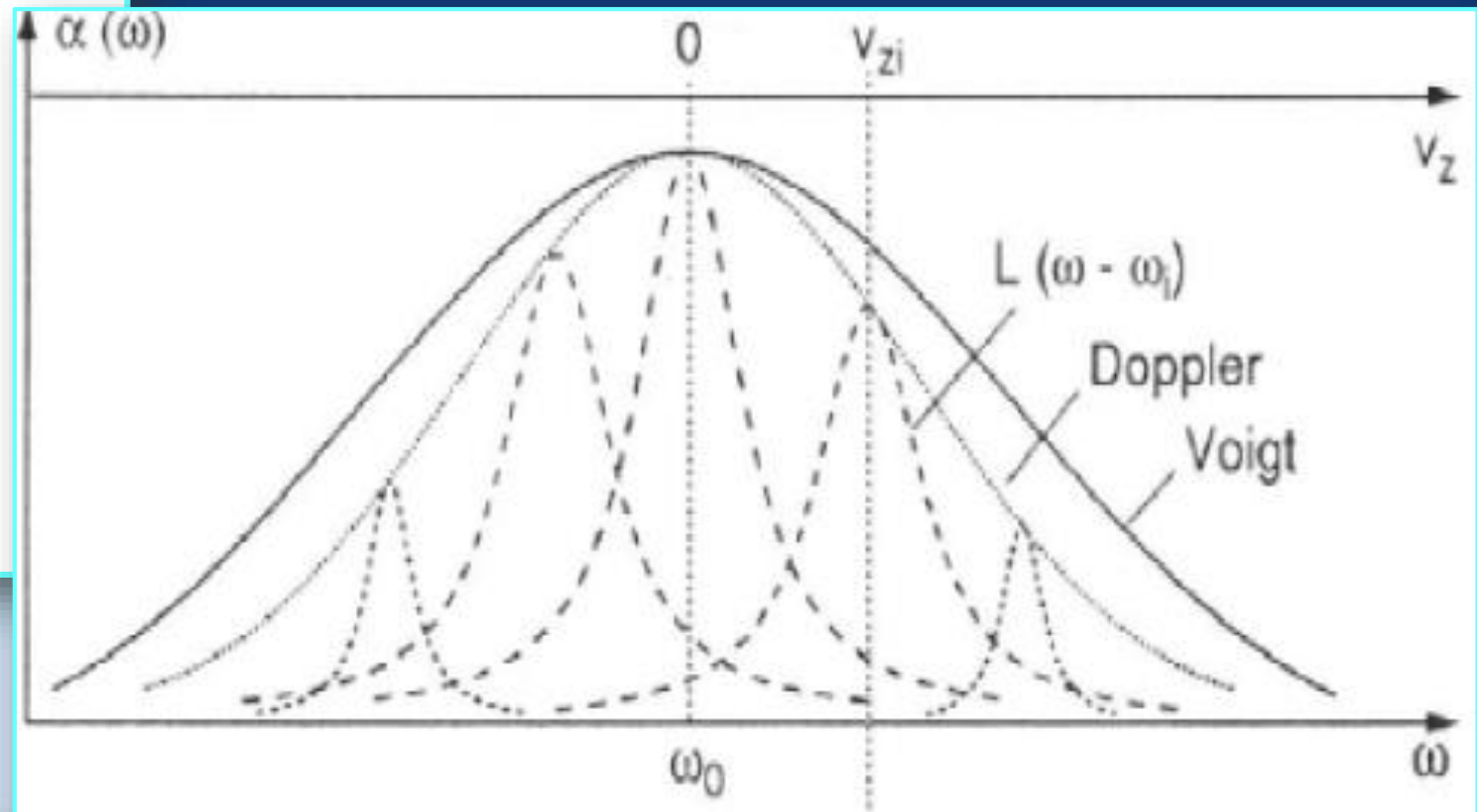
$$I_L(\sigma - \sigma_{fi}) = \frac{1}{\pi} \frac{\gamma_{fi}}{(\sigma - \sigma_{fi} - \delta_{fi})^2 + \gamma_{fi}^2}$$

- γ and δ proportional to the # of coll (dens or P)

The Voigt Profile



Comparison between the Gaussian, the Lorentz and the Voigt profiles.

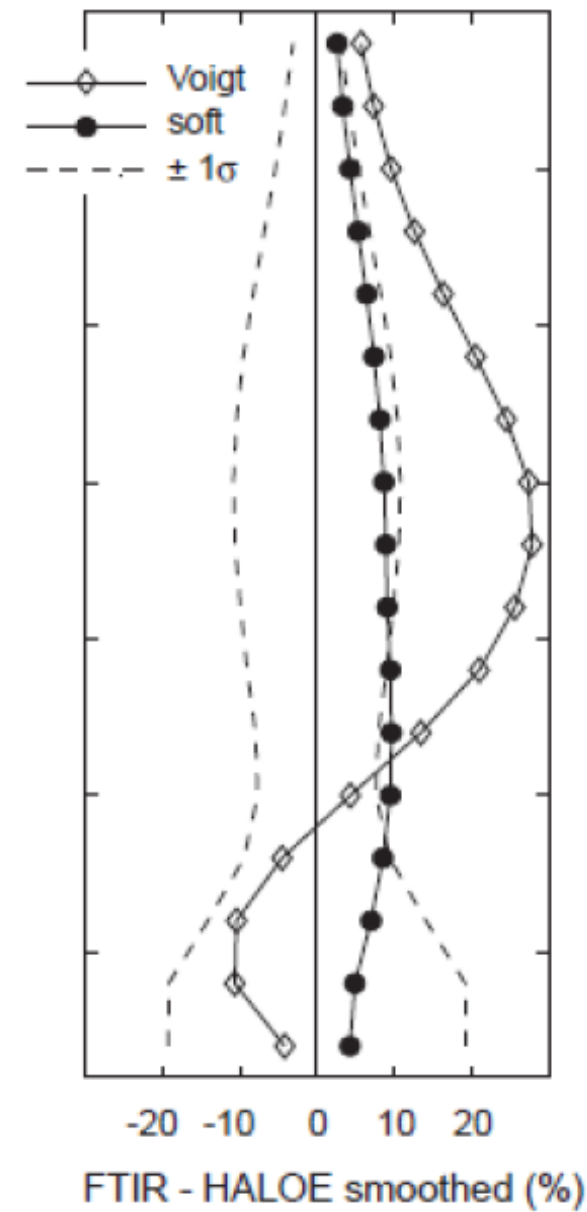
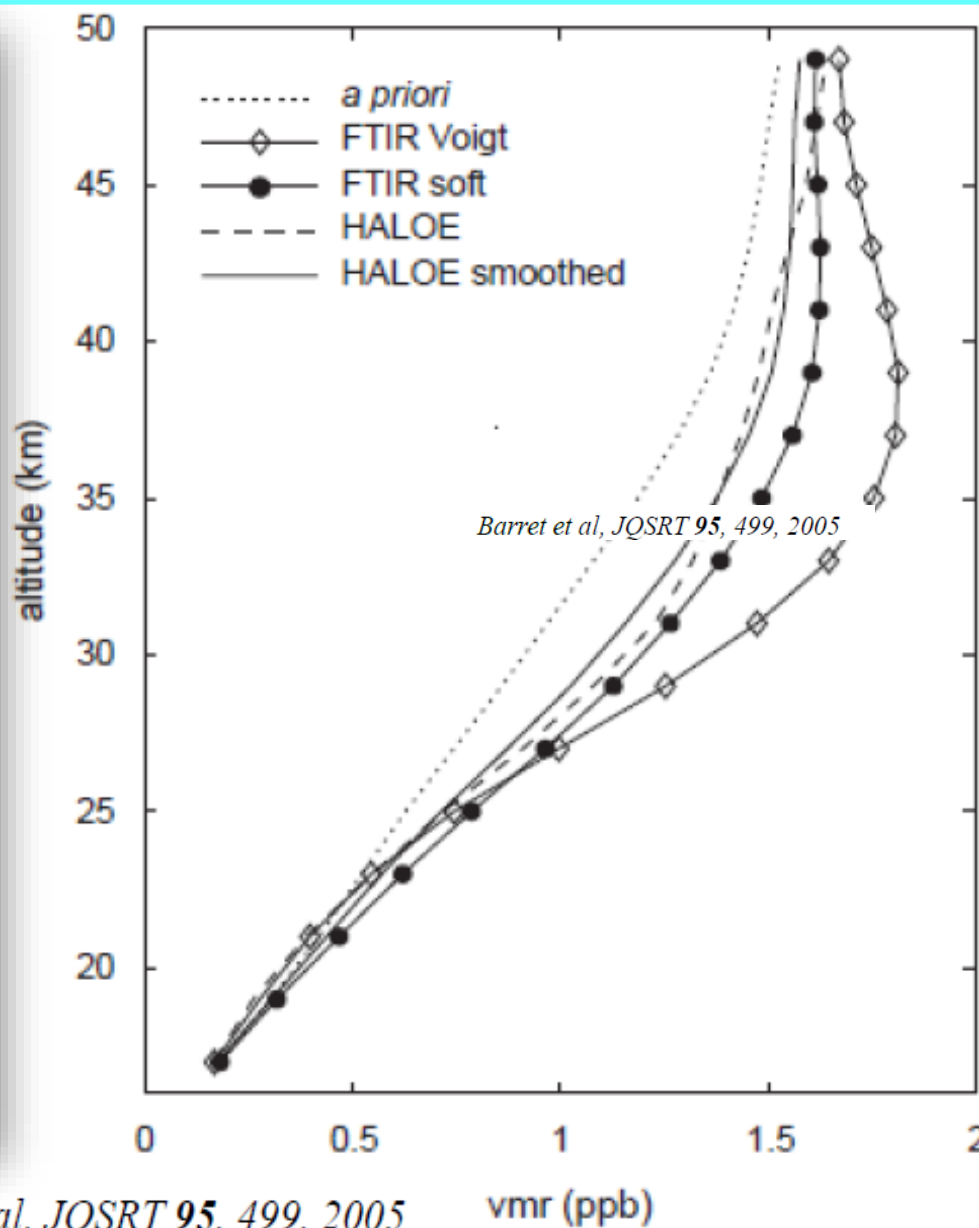
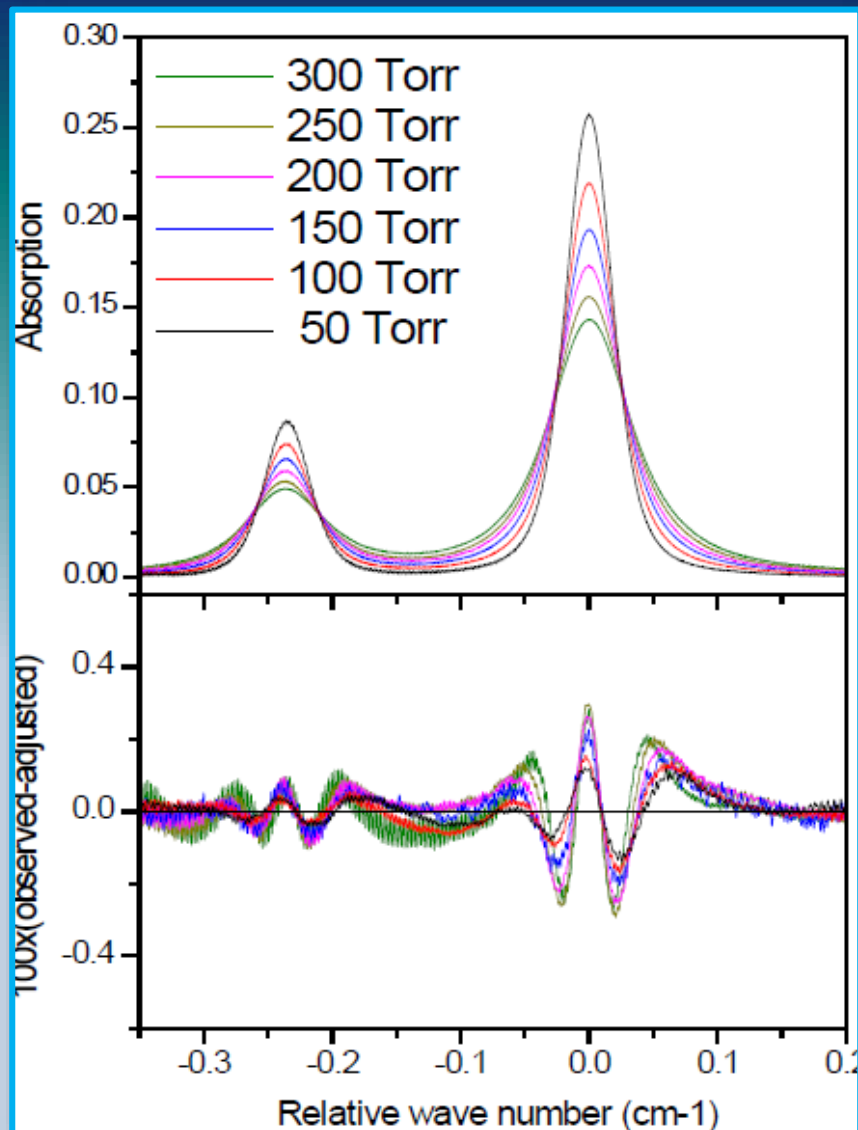


The resulting profile is then obtained by summing over all speed classes (or all σ')

$$I_V(\sigma - \sigma_{fi}) = \int_{-\infty}^{+\infty} d\sigma' I_D(\sigma' - \sigma_{fi}) I_L(\sigma - \sigma')$$

The Voigt profile is thus a convolution of a Gaussian profile (Doppler effect) and a Lorentzian profile (collisional effect).

Observed limitations of the Voigt profile



al, JQSRT 95, 499, 2005

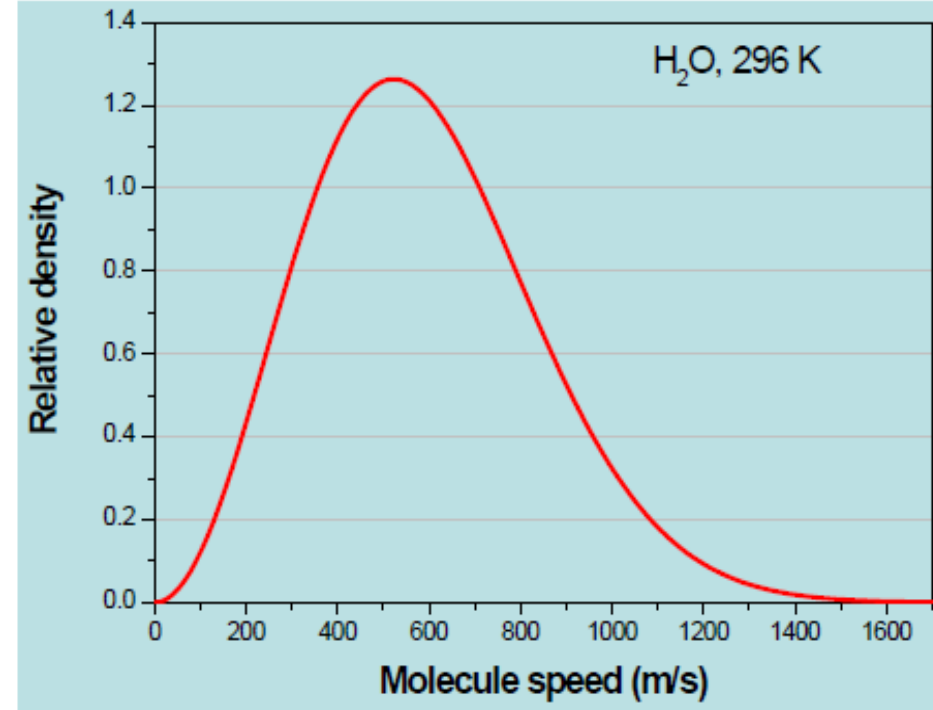
Why does the Voigt profile have limitations?

The Voigt profile neglects:

1. The velocity changes induced by collisions.

The detailed balance:

$$f(\vec{v} \rightarrow \vec{v}') \times f_{MB}(\vec{v}) = f(\vec{v}' \rightarrow \vec{v}) \times f_{MB}(\vec{v}')$$



→ change from v to $v' < v$ is more probable than that from v to $v' > v$.

→ reduction of the Doppler broadening → Dicke narrowing effect

2. The speed-dependences of the collisional width $\Gamma(v)$ and shift $\Delta(v)$ of the line.

This also (in general) leads to a narrowing of the line

Implementations of Speed Dependence in Spectral Line Profiles

- The polynomial dependence of Berman-Pickett

$$\Gamma(v_r) \propto v_r^p$$

$$\Gamma(v_a) = \int \Gamma(v_r) \cdot f(v_r | v_a) dv_r$$

Berman, *J. Quant. Spectrosc. Radiat. Transf.* 12, 1331 (1972)

- The quadratic dependence of Rohart

$$\Gamma(v_a) = \Gamma_0 + \Gamma_2 [(v_a / \bar{v})^2 - 3/2] \quad \text{with } \Gamma_0 = \langle \Gamma(v_a) \rangle_{v_a}$$

Rohart, Wlodarczak, Colmont, Cazzoli, Dore, Puzzarini, *J. Mol. Spec.* **251**, 282 (2008)

$m_{\text{active}} \gg m_{\text{buffer}}$

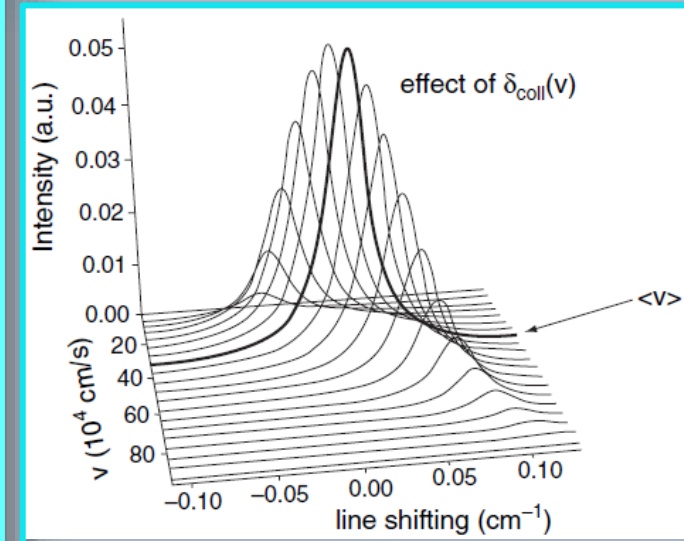
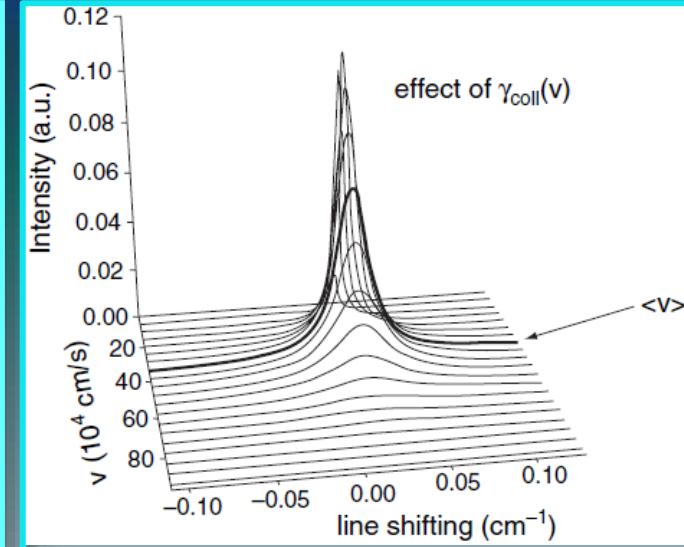
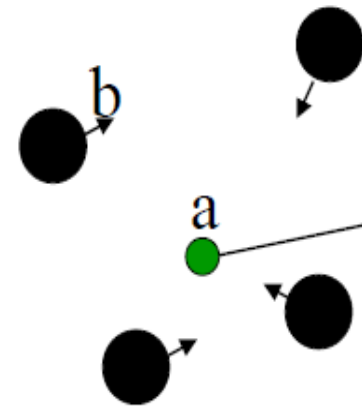
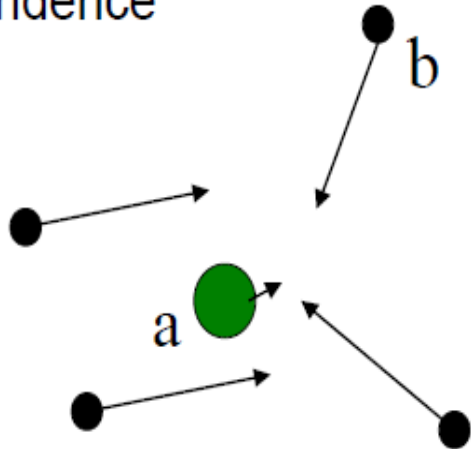
$m_{\text{active}} \ll m_{\text{buffer}}$

Weak speed dependence

Strong speed dependence

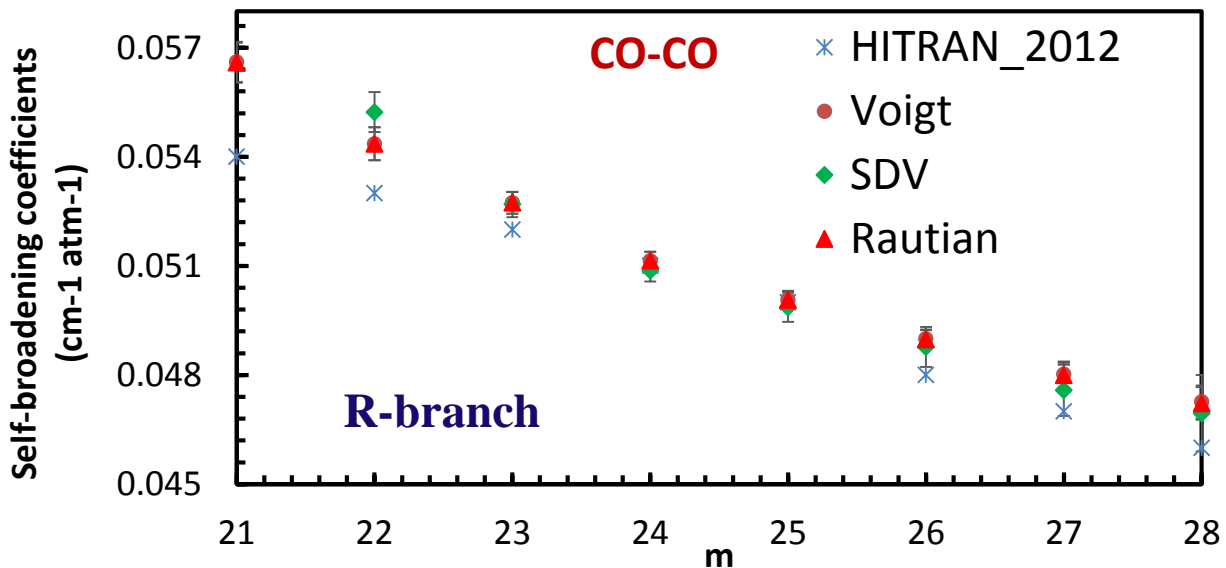
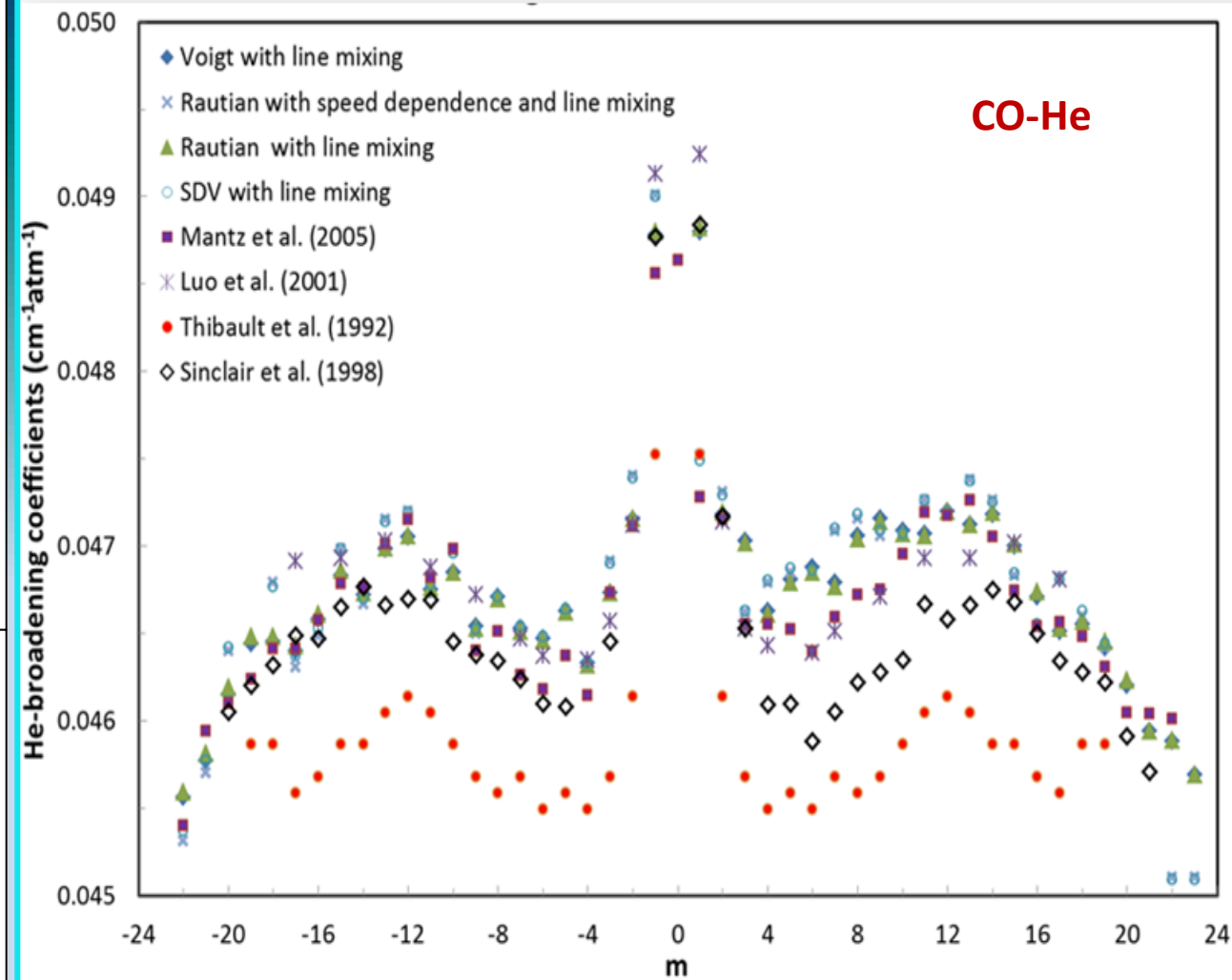
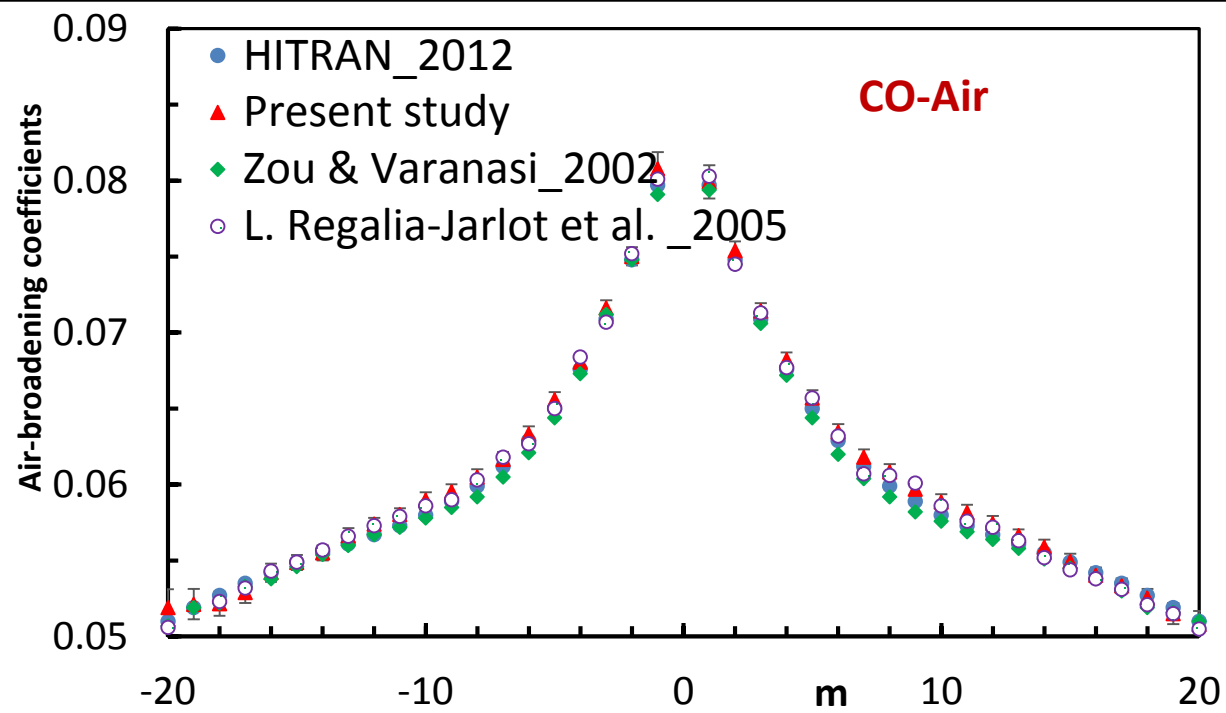
$$v_a \ll v_r \neq v_b$$

$$v_a \neq v_r \gg v_b$$

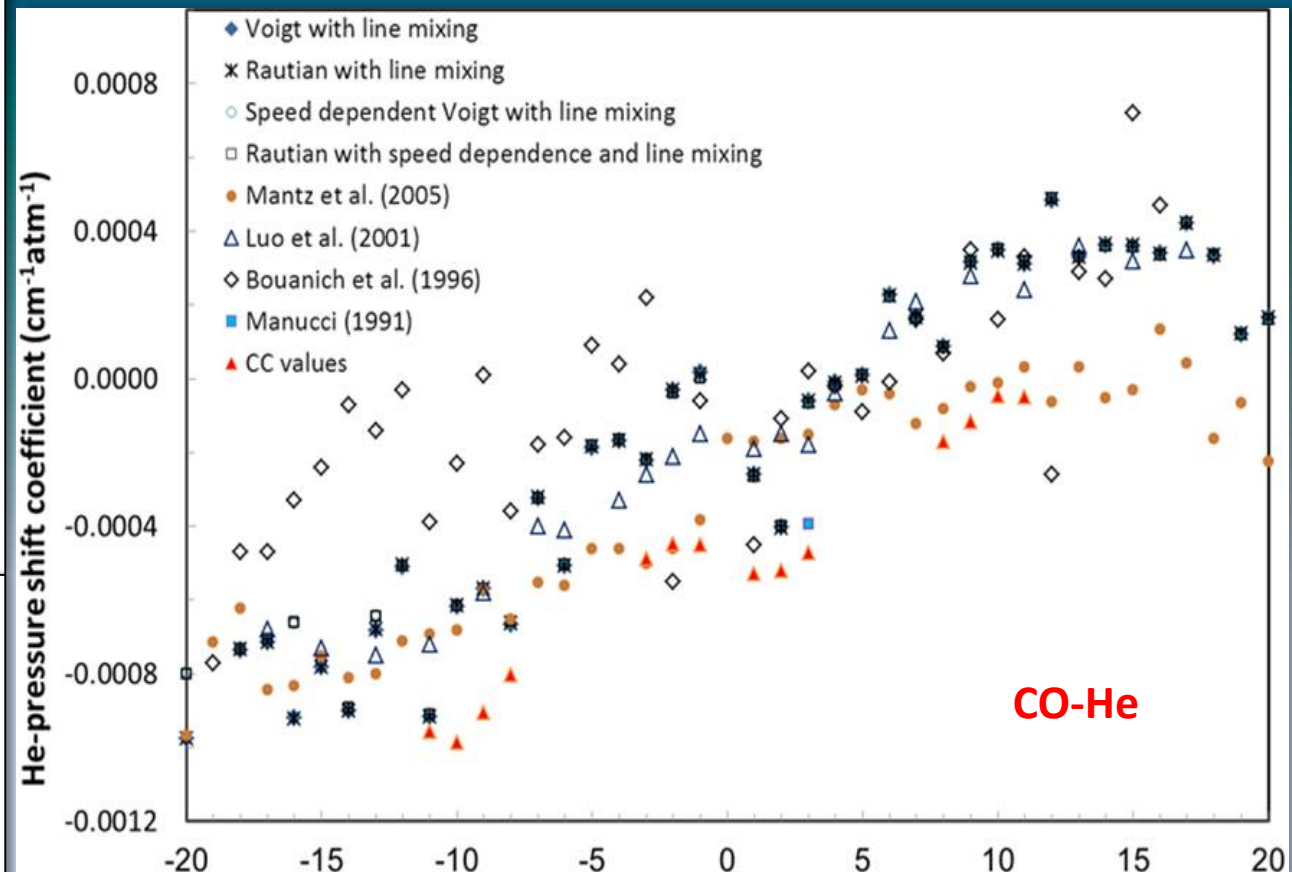
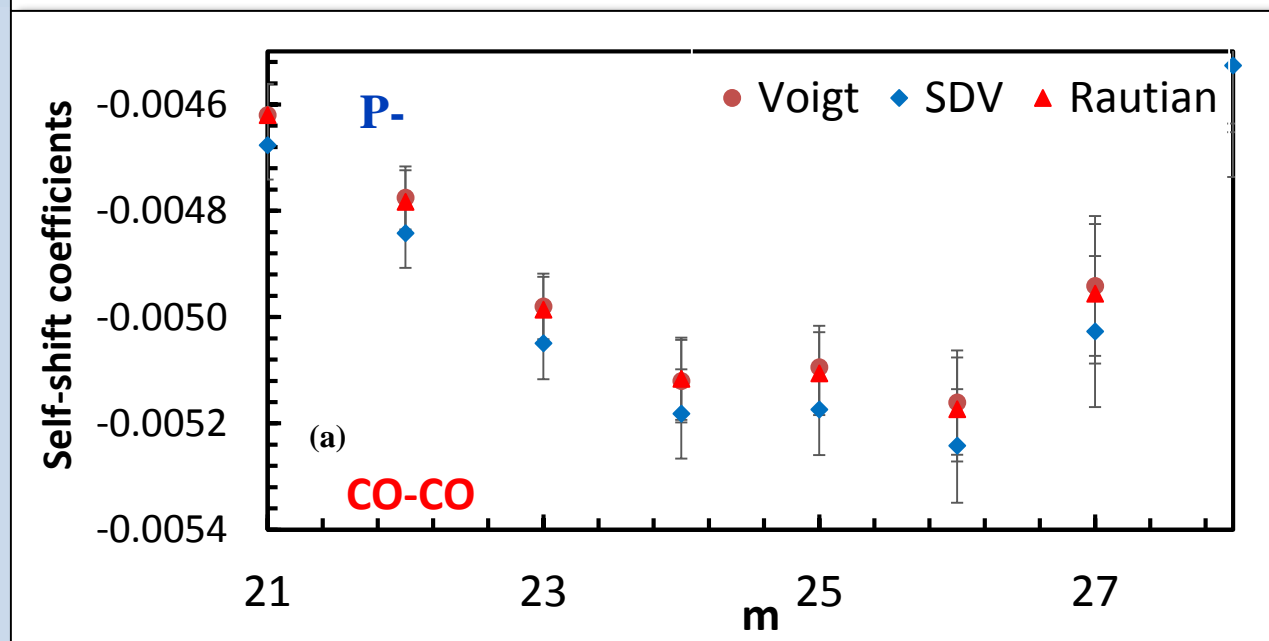
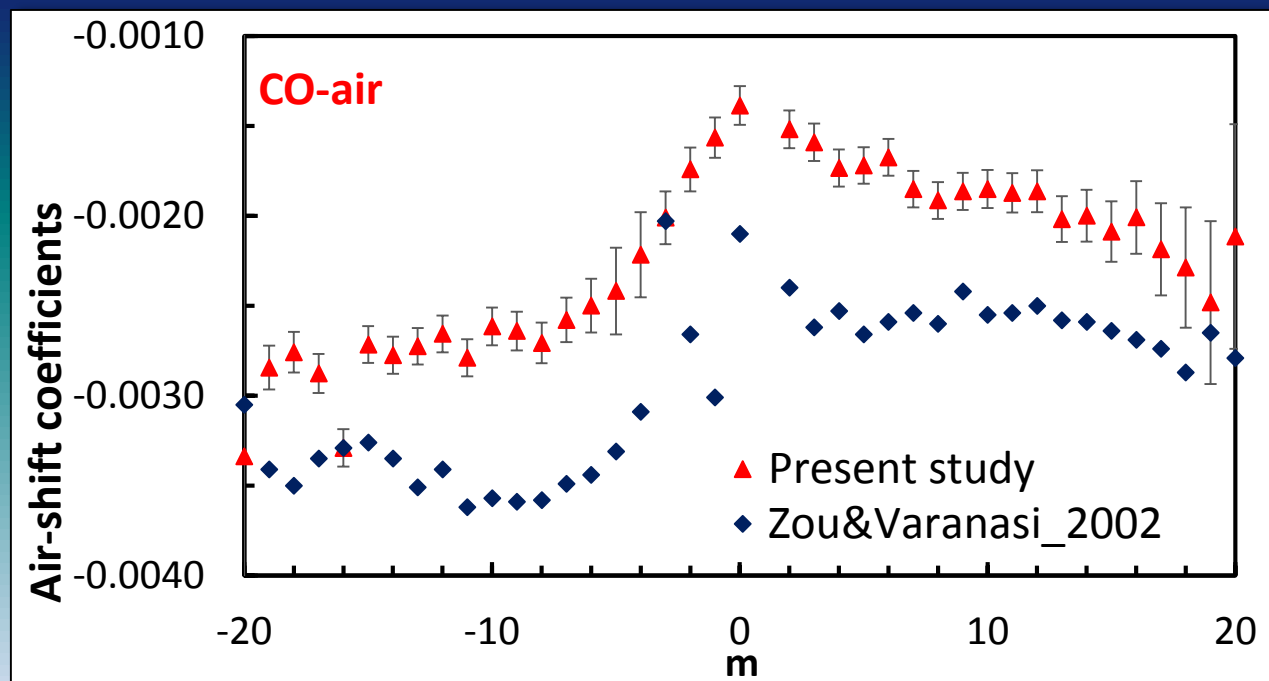


Ref. J.-M. Hartmann, C. Boulet, D. Robert, *Collisional Effects on Molecular Spectra* (2011).

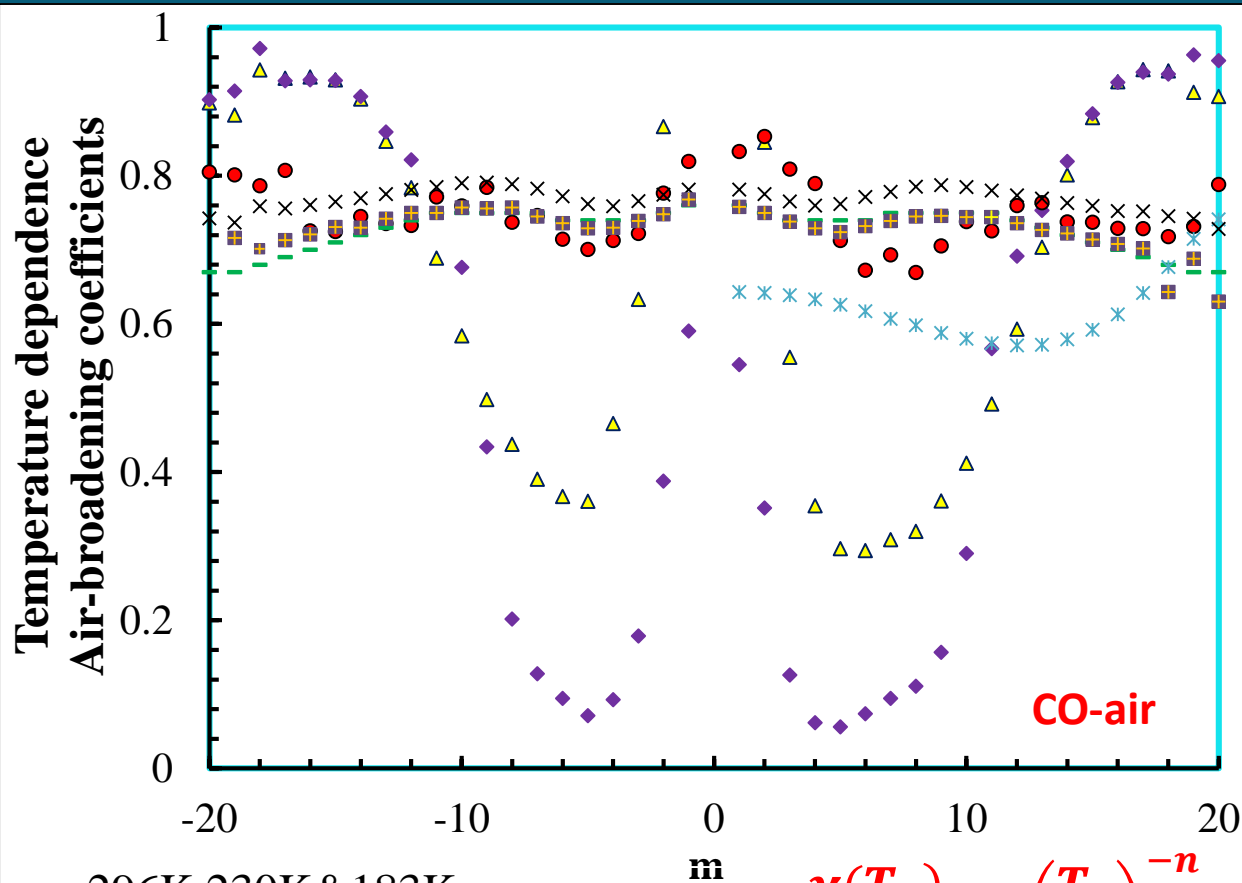
Broadening coefficients of CO broadened by CO, air, He at 296 K



Pressure-induced shift coefficients in the 1-0 band of CO at 296 K



Temperature dependences of air-broadening coefficients

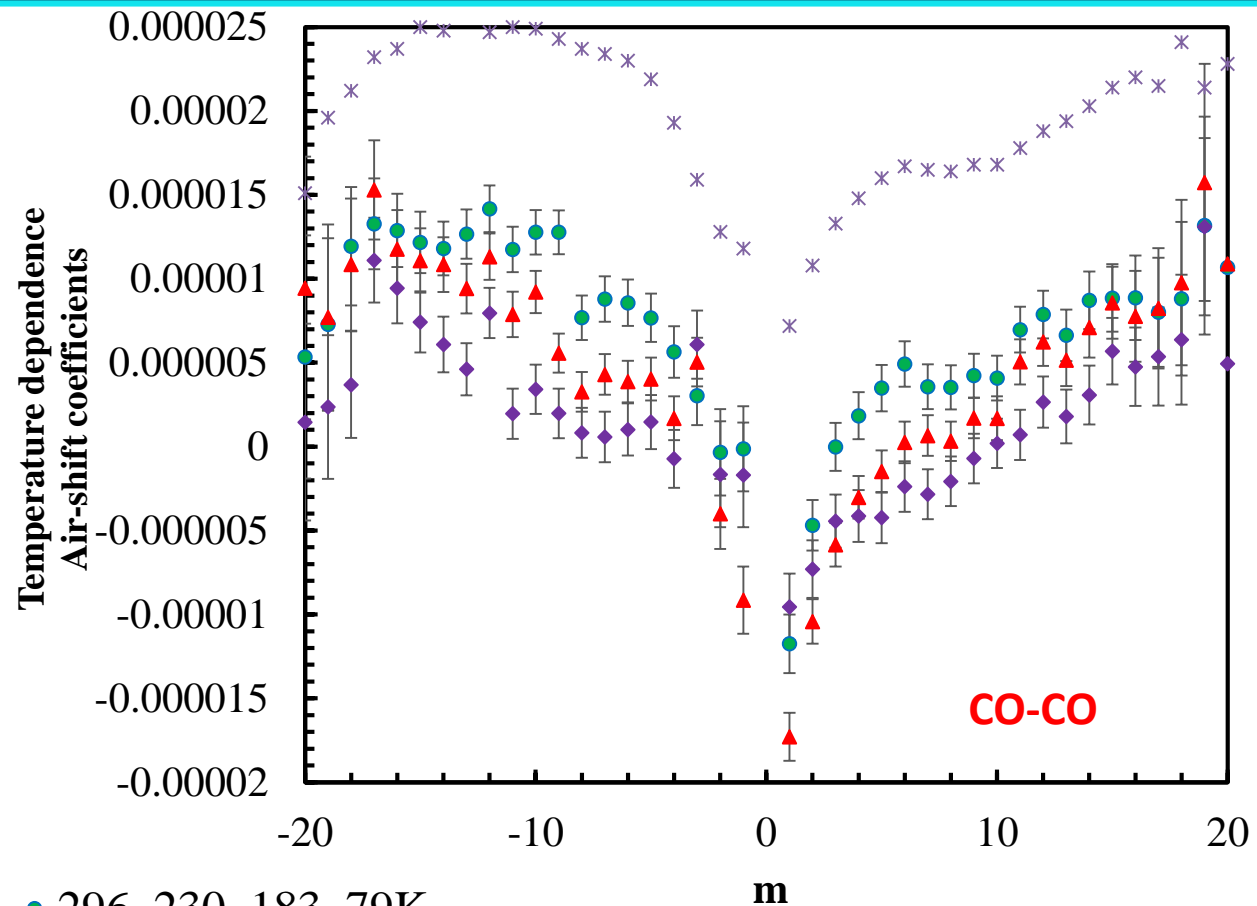


- ▲ 296K,230K&183K
- ◆ 296K,230K,183K&79K
- 296K & 230K
- Hitran_2004
- * Predoi-Cross et.al.(CO-N2)_0-2 band
- × Devi et al_2012 (0-2 band)
- Zou&Varanasi_2002

$$\frac{\gamma(T_1)}{\gamma(T_2)} = \left(\frac{T_1}{T_2}\right)^{-n}$$

n is the temperature-dependence broadening coefficient

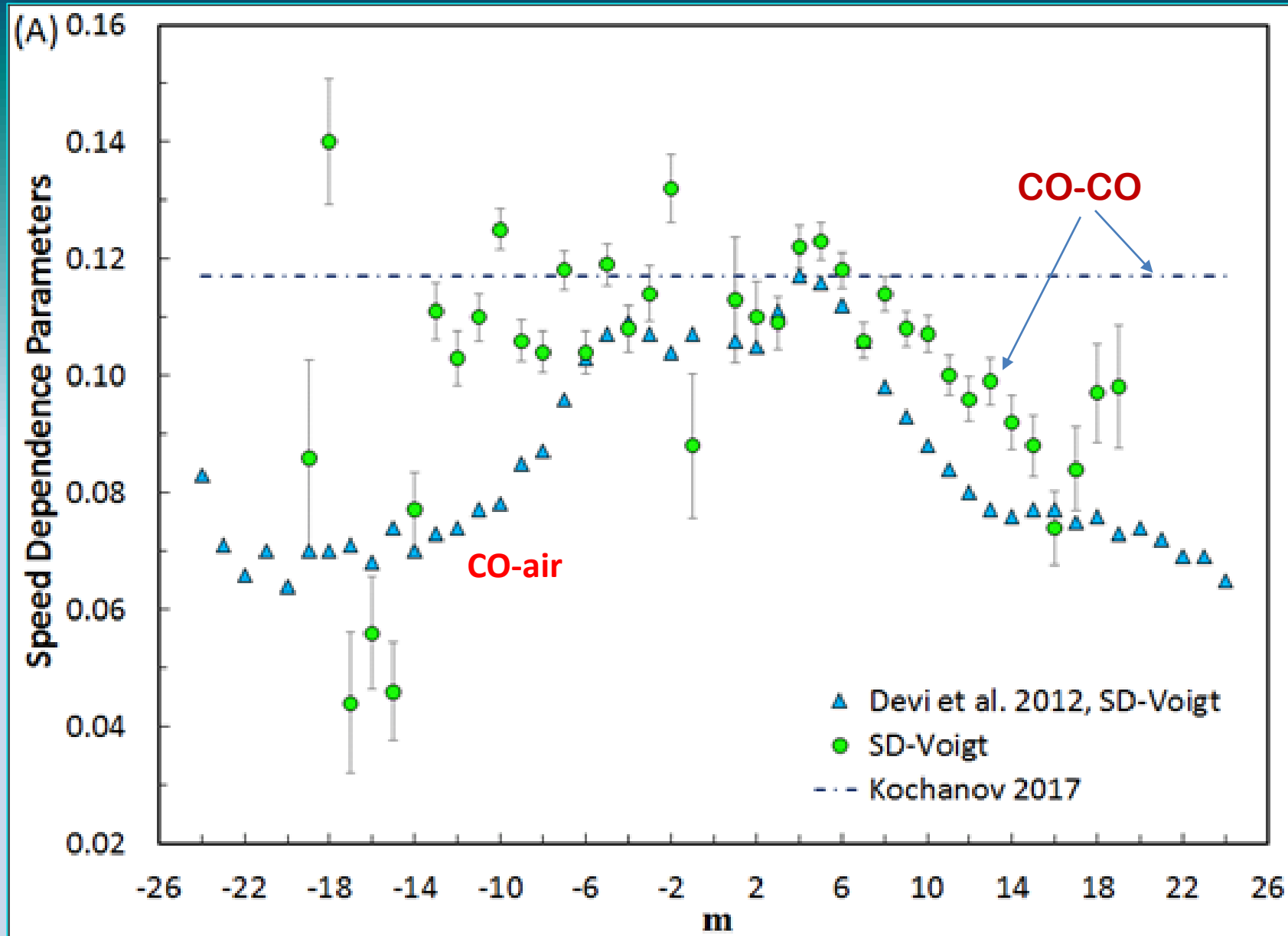
Temperature dependences of pressure induced air-shift



- 296_230_183_79K
- ◆ 296_230K
- ▲ 296_230_183K
- * Devi et al. 2012(0-2)

$$\delta_{He}^0(T) = \delta_{He}^0(T_0) + \delta'_{He} \times (T - T_0)$$

Speed dependence parameters for CO-CO and CO-air mixtures obtained using the speed-dependent Voigt profile.



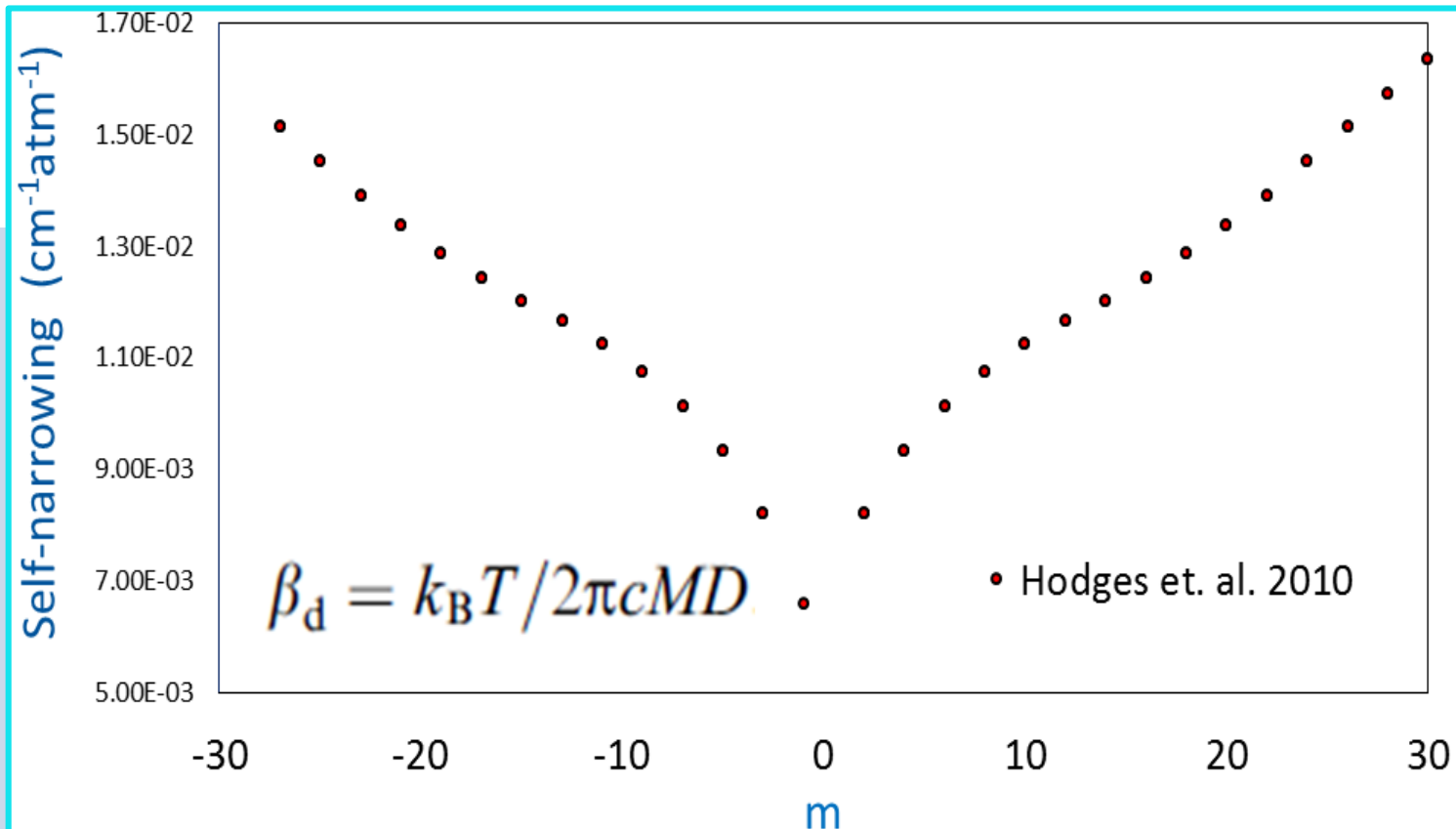
Dicke Narrowing

If the mean free path of the molecules becomes equal to, or less than to the wavelength of the incident radiation λ , the resulting motion of the molecules becomes Brownian in nature and the gas diffusion becomes relevant.

Lineshapes that account for the effect:

- (1) **Galatry** profile incorporates the Brownian movement model and assumes only small changes in the radiators velocity during collisions (*soft collisions*).
- (2) **Nelkin-Ghatak** profile and the **Rautian-Sobelman** model. For this line shapes each collision erases any information about the radiators velocity. This randomizes the velocities of the radiators i.,e. we have *hard collisions*.

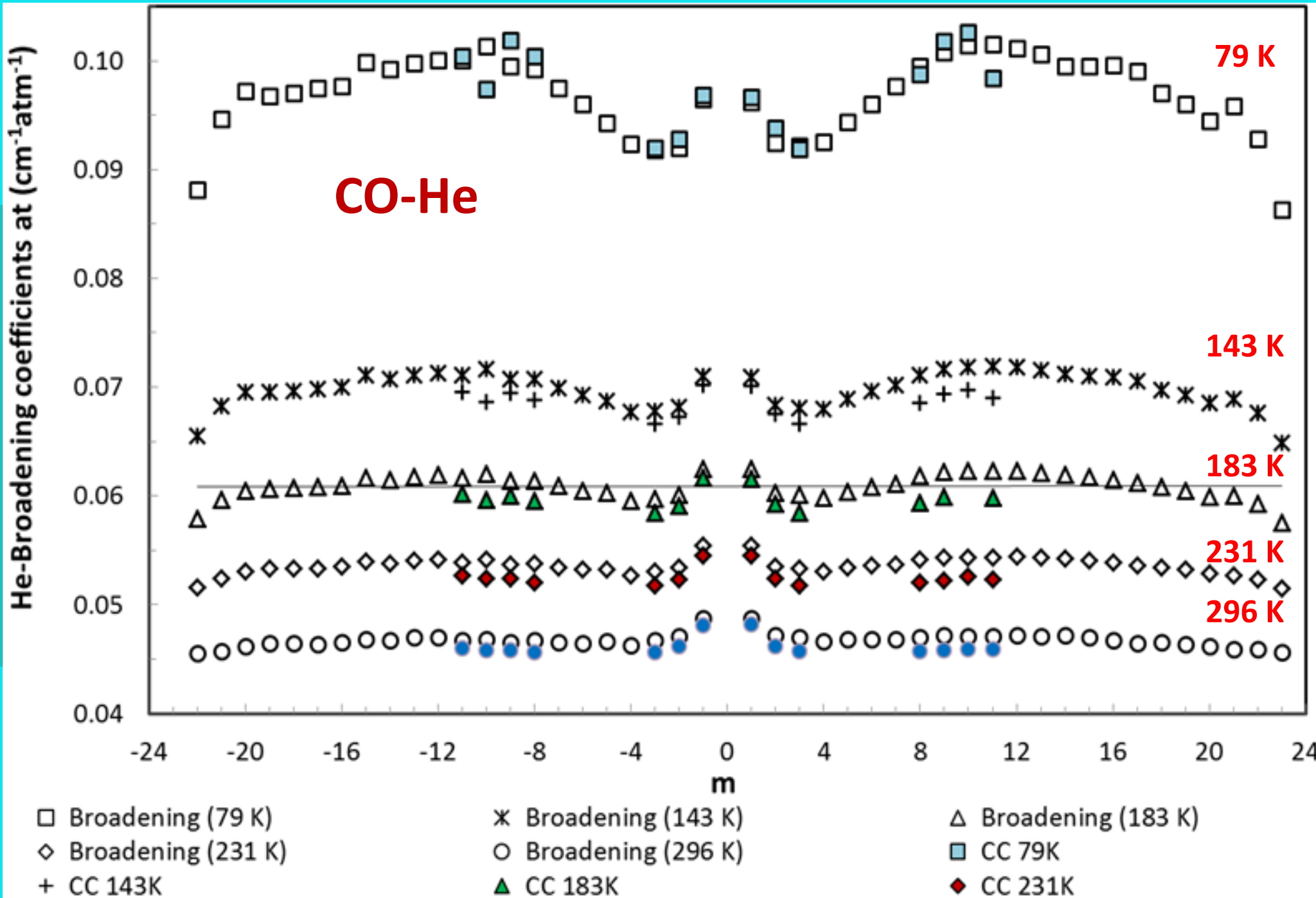
$$\varphi_{DP}(\nu) = \left(\frac{1}{\pi} \right) \frac{\gamma_o P + k^2 D_o / P}{(\nu - \nu_o - \delta_o P)^2 + (\gamma_o P + k^2 D_o / P)^2}$$



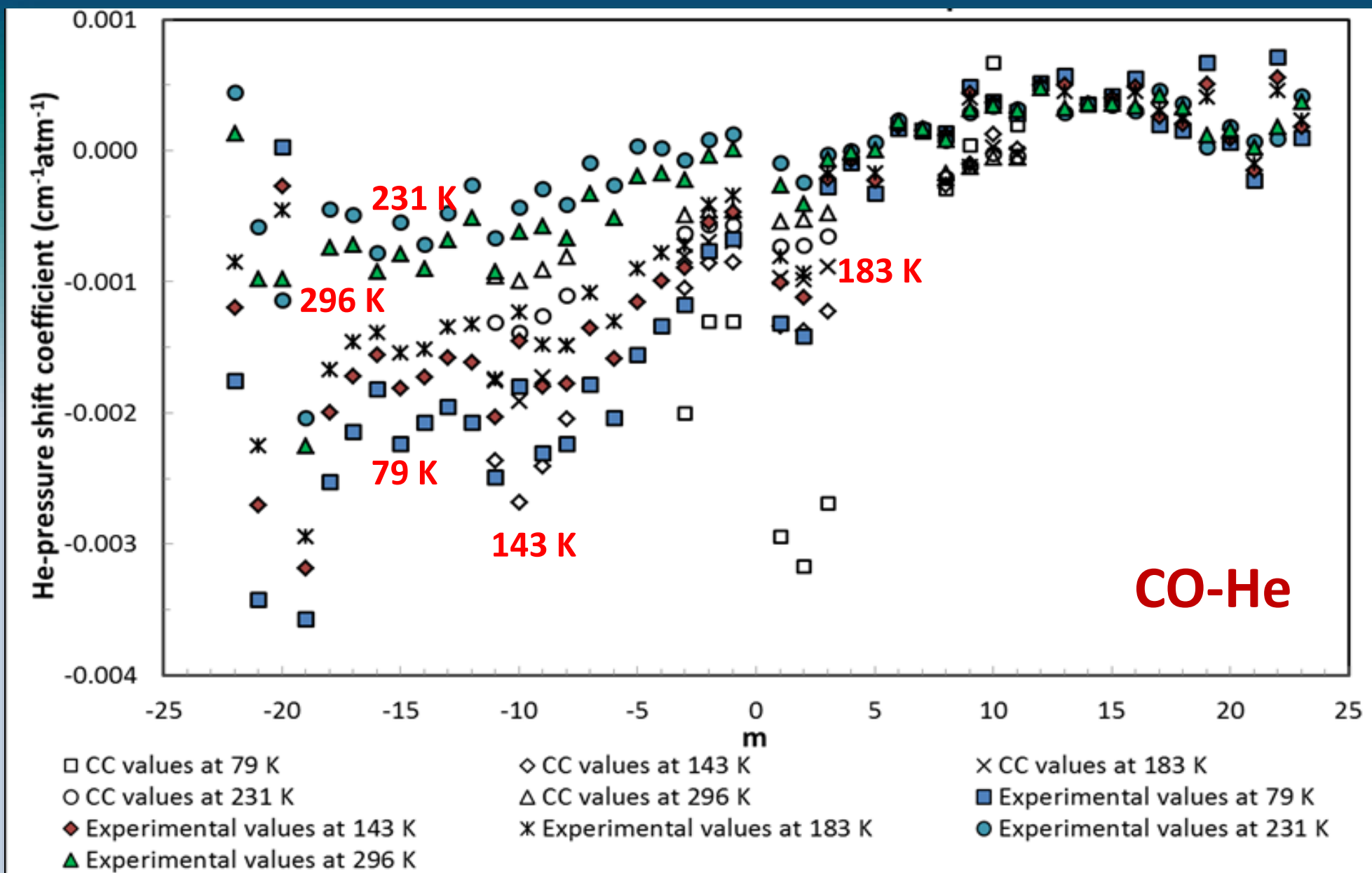
Close-coupled theoretical calculations of broadening, shift, narrowing coefficients applied to the $^{12}\text{C}^{16}\text{O}$ -He system

- The 3-D potential energy surface (PES) used was proposed by Heijmen *et al.* J. Chem. Phys. (1997).
- Most of the close-coupling pressure-broadening and shift cross-sections as a function of the relative collisional energies were the same as in Luo *et al.* J. Chem. Phys. 115 (2001).
- Additional calculations were devoted to purely rotational R lines to predict the odd component of the ro-vibrational shifts.
- Assuming that the even component of the shifts has a purely vibrational origin resulting from the isotropic parts of the PES and is therefore J-independent, we are able to retrieve the shift coefficients in the fundamental (at least at room T).
- Moreover, since the half width at half maximum is nearly vibrationally independent, we thus also present some results of our calculations performed in the vibrational ground state to complete our data analysis.

Experimental and theoretical (CC) broadening coefficients at different temperatures for CO-He



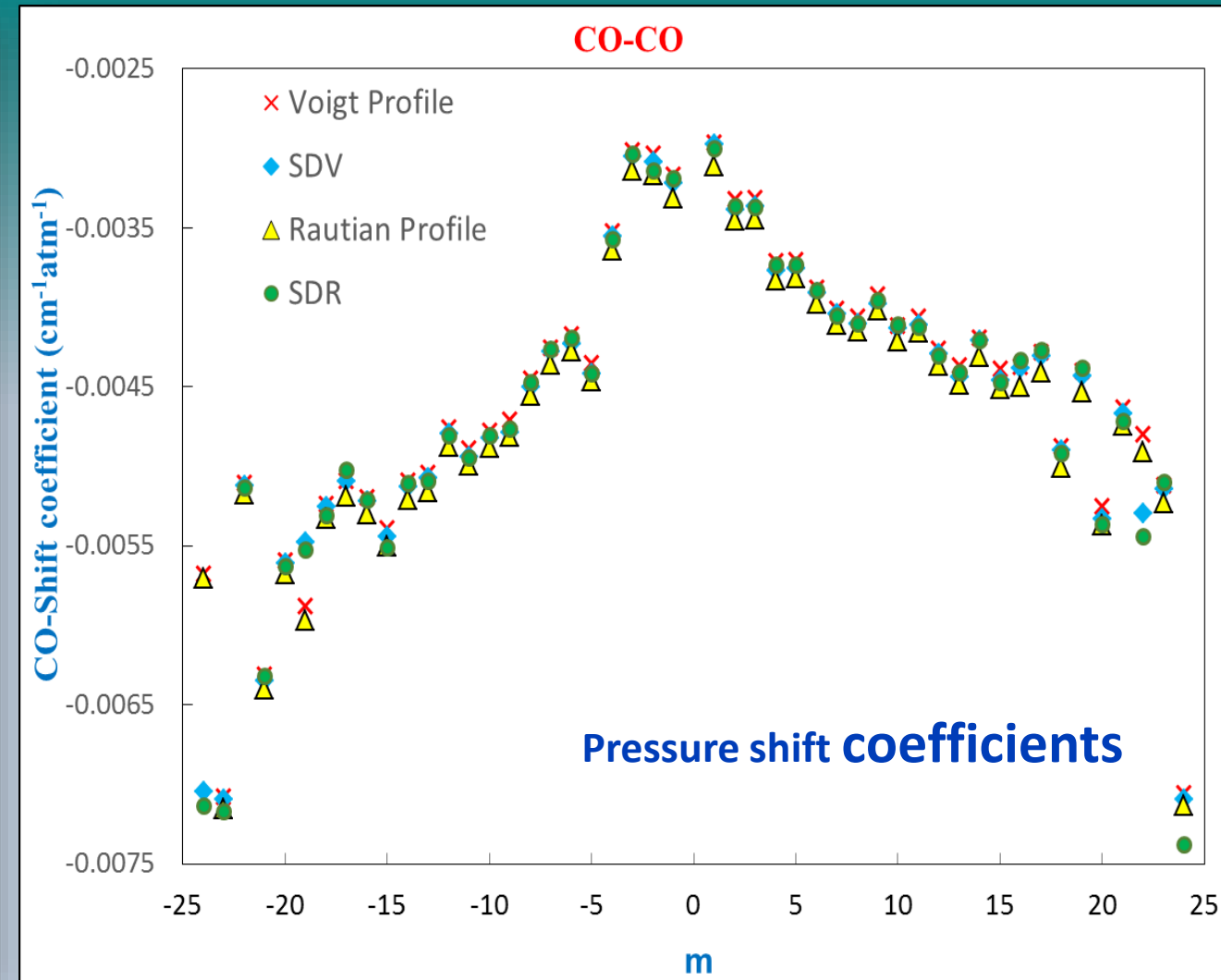
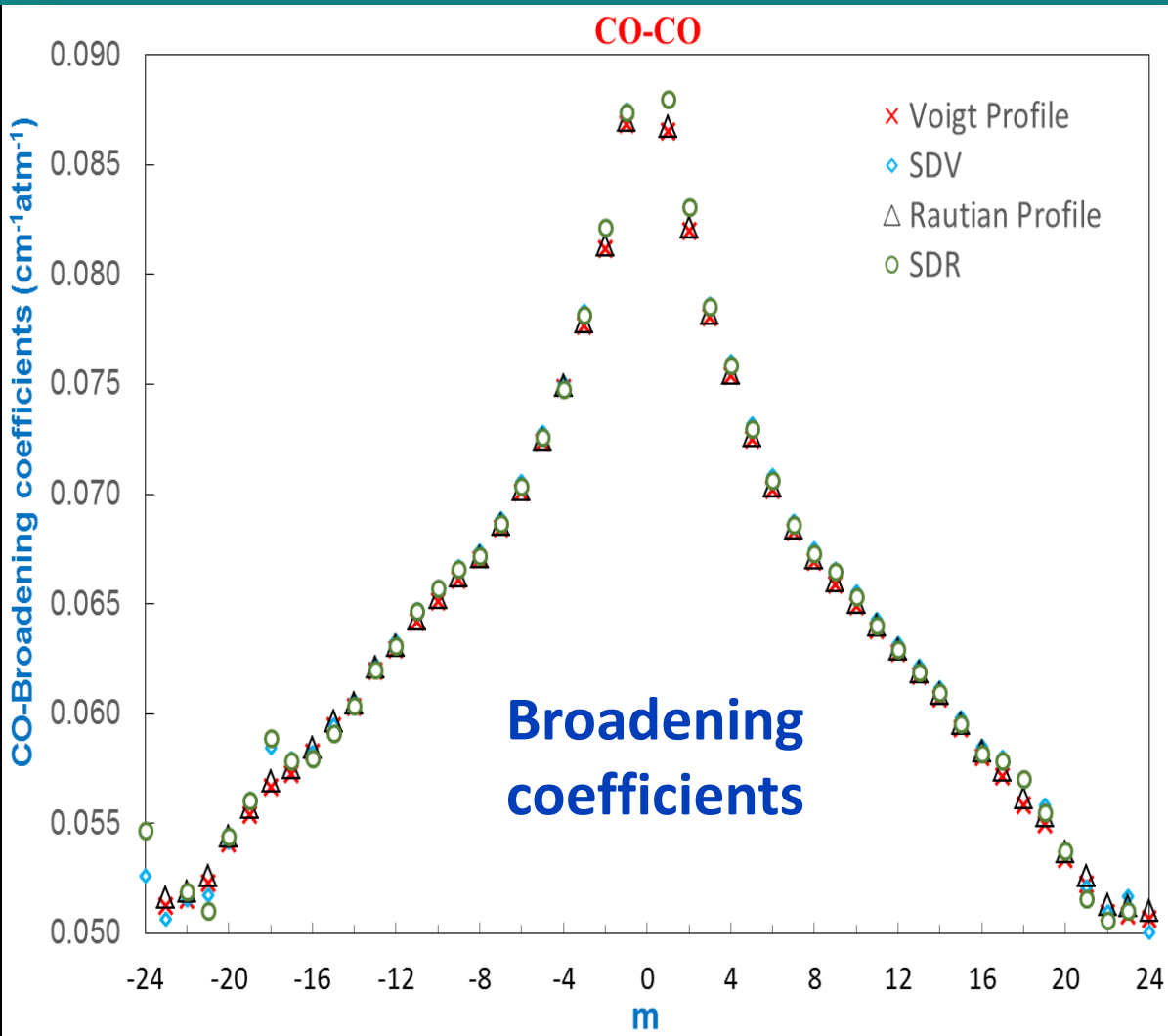
Experimental He-shift coefficients and the close coupled (CC) theoretical He-shifts at different temperatures.



Theoretical calculations of diffusion constants for the CO-CO system

- To estimate the mass diffusion of CO , the molecule was described from a three electrostatic sites model [A. Martín-Calvo et al., J. Phys. Chem. C **116** (2012)].
- Intermolecular interactions were described by combining electrostatic and van der Waals interactions.
- Molecular dynamics (MD) simulations were carried out from DLPOLY software.
- In the canonical ensemble, the temperature was kept constant by means of Nose-Hoover algorithm such that the relaxation time of the thermostat was 0.5 fs.
- The integration of motion equations was performed by using the velocity Verlet algorithm [M.P. Allen, D.J. Tildesley, Computer Simulation of Liquids, Oxford University Press, United states (1987)].

The theoretical narrowing parameters calculated using the diffusion constants presented here are currently used in our line parameter retrievals using the Rautian and speed-dependent Rautian models. Results for CO-CO are presented here.



Theoretical classical calculations of broadening coefficients of CO absorption lines

The calculations utilize simple vibrationally independent intermolecular interaction potential (Tipping-Herman + electrostatic). Both molecules are treated as rigid rotors. The dependences of CO half-width coefficients on rotational quantum number J , for $J \leq 24$ are computed and compared with measured data at room temperature.

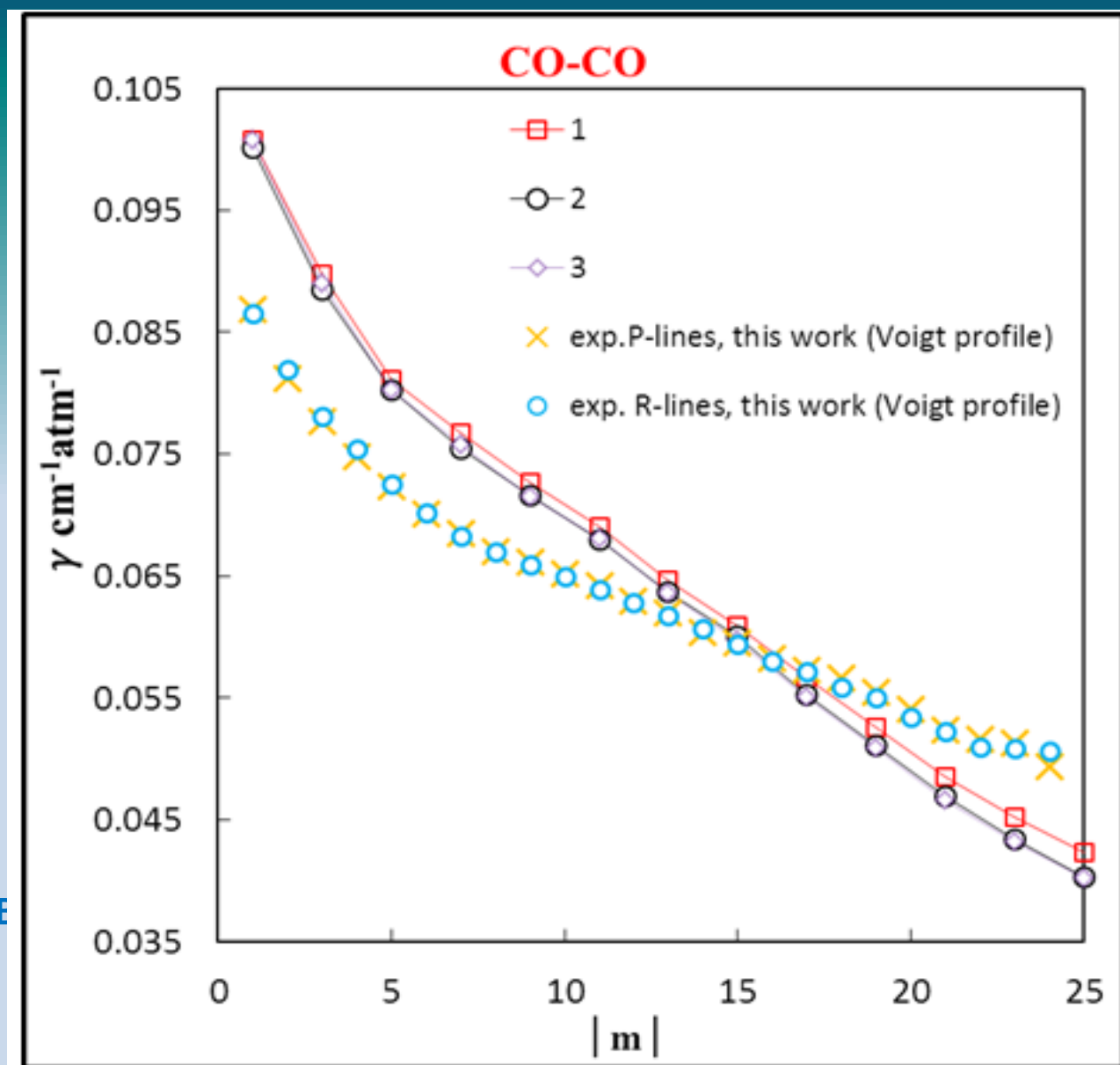
Molecular parameters for CO and H₂

Molecule	$r(\text{\AA})$	$B(\text{cm}^{-1})$	$\mu(\text{D})$	$Q(\text{D}\cdot\text{\AA})$
¹² C ¹⁶ O	1.1309	1.9225	0.11	-2.0

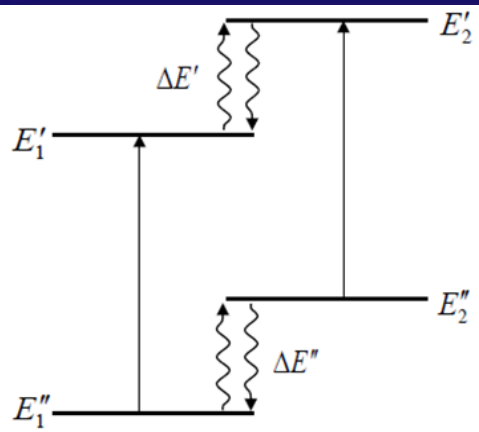
Lennard – Jones interaction parameters, ϵ , σ

Interaction	$\epsilon(\text{K})$	$\sigma(\text{\AA})$
CO-CO	110	3.59
	91.7	3.69

Theoretical classical calculations of broadening coefficients of CO absorption lines obtained using 3 sets of potential parameters



Line Mixing Effects



At elevated pressures molecular collisions induce transfers of populations between the levels of the two absorption lines that lead to transfers of intensity between the lines.

Absorption Coefficient $\alpha^{\text{LM}}(\sigma) \propto \sum_{\text{line } \ell} \sum_{\text{line } k} \rho_{\ell} d_{\ell} d_k \langle k | [\Sigma - L_0 - iPW]^{-1} | \ell \rangle$

ρ_k populations


d_k matrix element of radiation-matter coupling tensor

Σ, L_0 matrix of positions

W **relaxation operator**. All effects of collisions. Independent of σ within the impact approximation (not too far in the wings)

$W_{lk} \neq 0 \rightarrow$ Line coupling between $|k\rangle$ and $|l\rangle$

$W_{lk} = 0 \rightarrow$ No line coupling (Lorentz)

 $\alpha^{\text{Lo}}(\sigma) \propto \sum_k \rho_k d_k^2 \times \left[\frac{\gamma_k}{(\sigma - \sigma_k - \delta_k)^2 + \gamma_k^2} \times \frac{1}{\pi} \right]$

$$\langle k | W | k \rangle = \Gamma_k - i\Delta_k$$

Det. Balance: $\rho_l \langle k | W | l \rangle = \rho_k \langle l | W | k \rangle$

Sum rule: $\sum_{\text{lines } l} d_l \langle l | W | k \rangle = 0$

$$Y_k = 2 \sum_{l \neq k} \frac{d_l}{d_k} \frac{W_{kl}}{\sigma_k - \sigma_l}$$

Scaling Laws

Exponential Power Gap Model

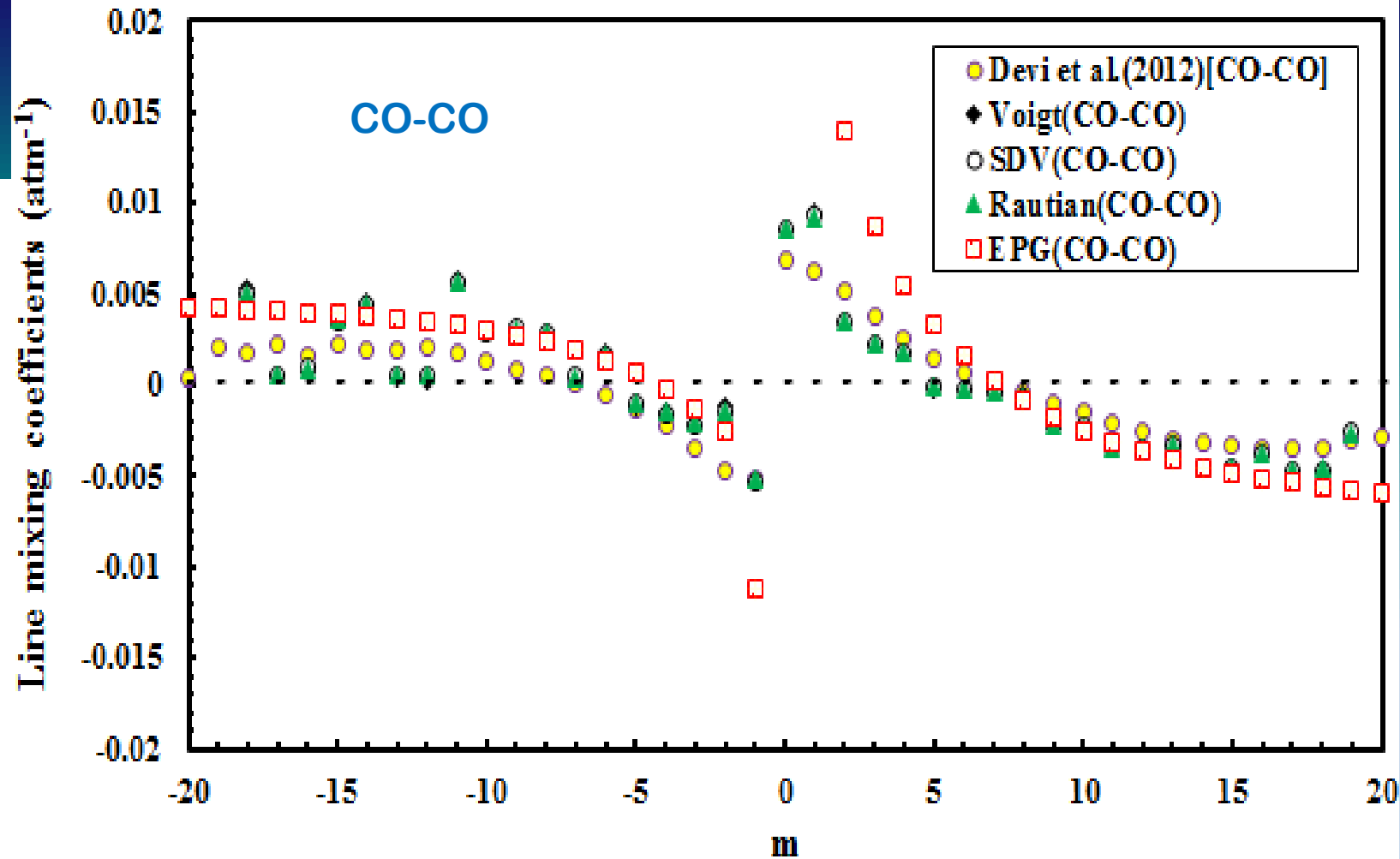
To find the relaxation matrix we use a nonlinear Marquardt algorithm to optimally fit the parameters a, b and c in the state to state transfer equation.

The best fit is found by optimizing the diagonal elements of the relaxation matrix to be equal to the experimentally determined broadening coefficients.

$$\kappa_{jk} = a \left[\frac{|\Delta E_{jk}|}{B_0} \right]^{-b} \exp \left(\frac{-c |\Delta E_{jk}|}{B_0} \right)$$

$$Y_k = 2 \sum_{j \neq k} \frac{d_j}{d_k} \frac{W_{jk}}{v_k - v_j}$$

Optimized adjustable parameters for the EPG scaling law. \Rightarrow



β	Values (CO-CO)	Parameters	Values (Air-CO)	β
	0.04219332(3)	a	0.02970517(4)	
0.6	0.45056420(6)	b	0.35939840(6)	0.55
	1.02971900(7)	c	1.098497009(8)	

Energy Corrected Sudden (ECS) Approximation

This is a dynamically based scaling law that takes into account the finite durations of collisions through the addition of an adiabaticity factor.

- The elements of the relaxation matrix are calculated from the following function.

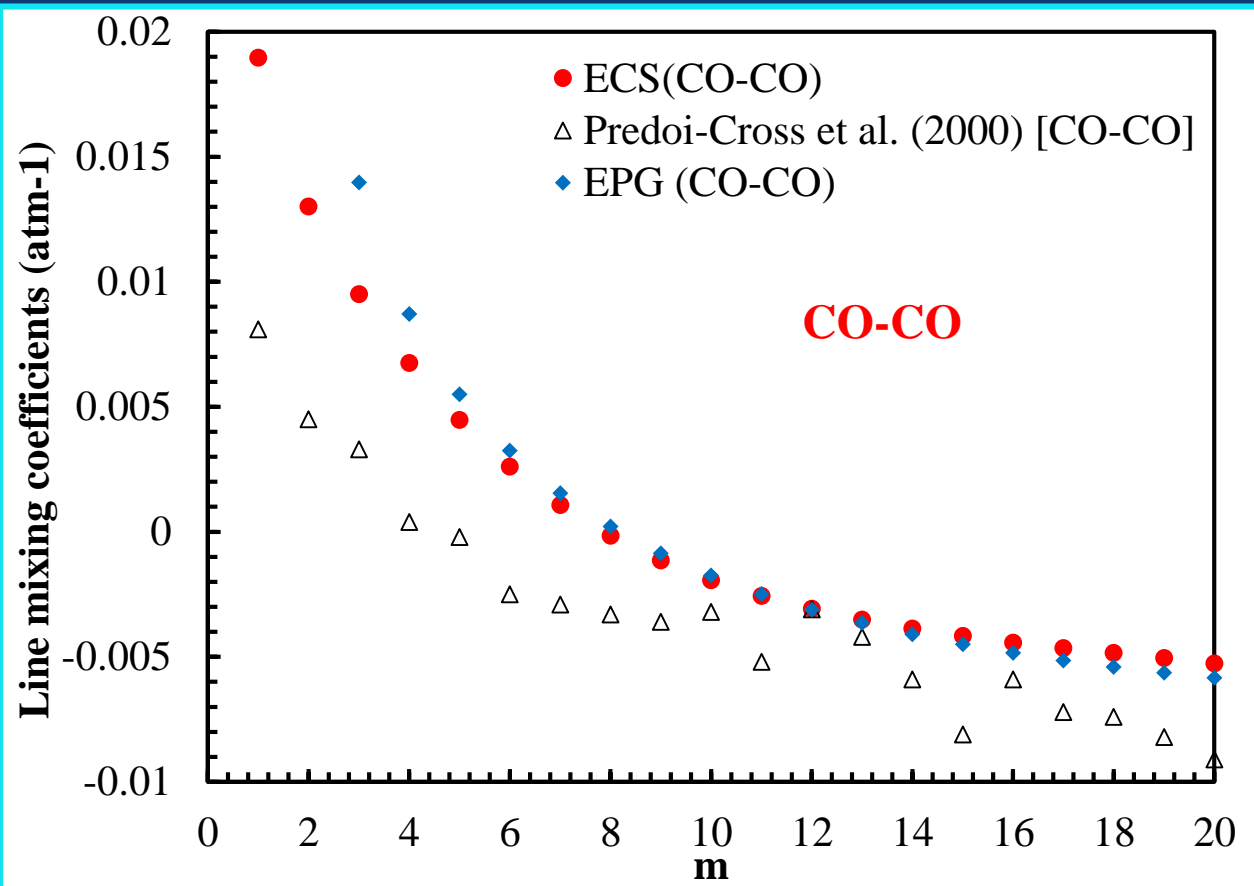
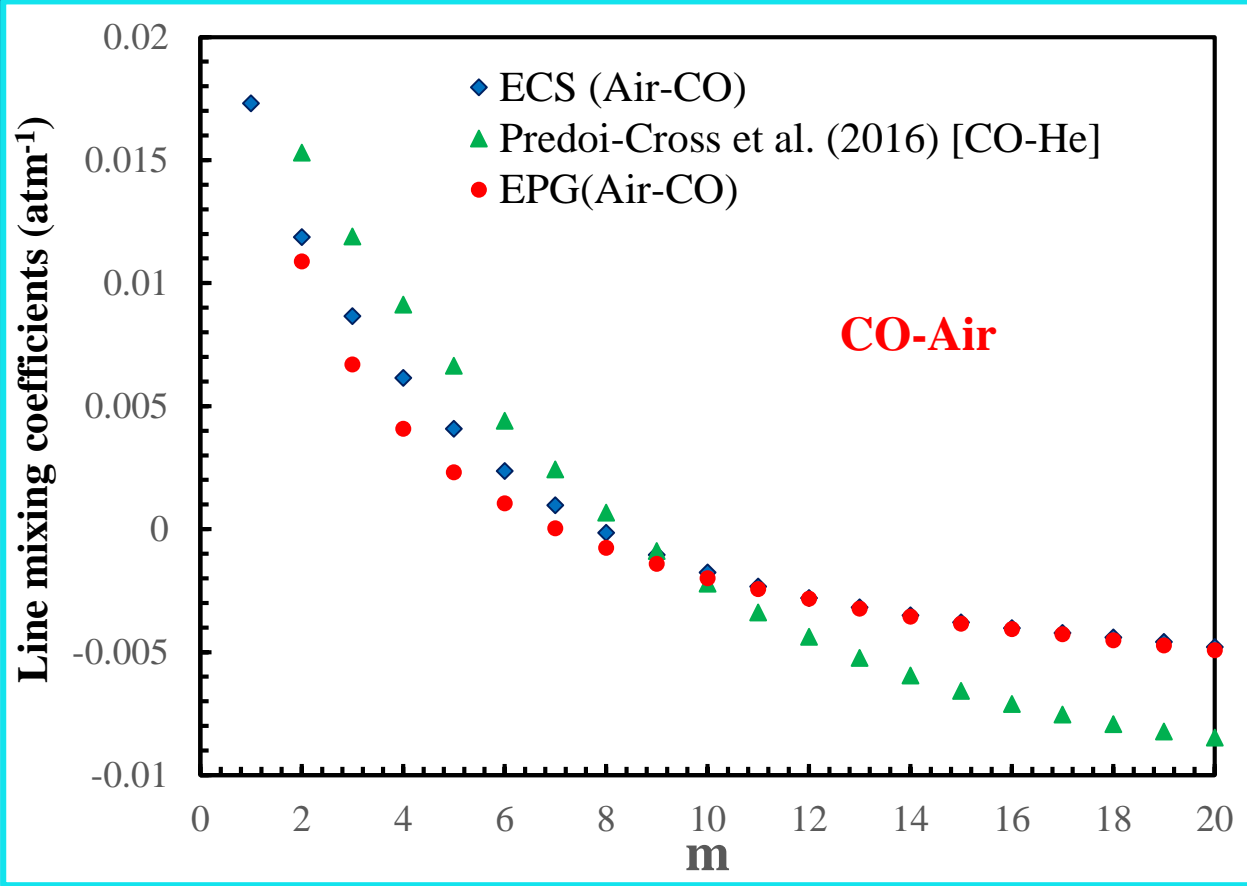
$$\langle J_i' J_f' | W(T) | J_i J_f \rangle = (2J_i' + 1) \sqrt{(2J_f + 1)(2J_f' + 1)} \\ \times \sum_{L \text{ Even} \neq 0} \begin{pmatrix} J_i & L & J_i' \\ 0 & 0 & 0 \end{pmatrix} \begin{pmatrix} J_f & L & J_f' \\ 0 & 0 & 0 \end{pmatrix} \begin{Bmatrix} J_i & J_f & 1 \\ J_f' & J_i' & L \end{Bmatrix} \times (2L + 1) \frac{\Omega_J}{\Omega_L} Q_L$$

$$\Omega_J = \left\{ 1 + \frac{1}{24} \left[\frac{\Delta\omega_j d_c}{\bar{v}} \right]^2 \right\}^{-2} \\ \Omega_L = A \left[\frac{E_L}{B} \right]^{-\lambda} \exp \left(-\beta \frac{E_L}{K_B T} \right)$$

$$Y_k(T) = 2 \sum_{j \neq k} \frac{d_j}{d_k} \frac{W_{jk}}{v_k - v_j}$$

$\Delta\omega_j$ is the energy difference between the rotational energy levels. d_c, \bar{v}, E_L, B are the scaling length, mean relative velocity in CO-Air collisions, rotational constant respectively.

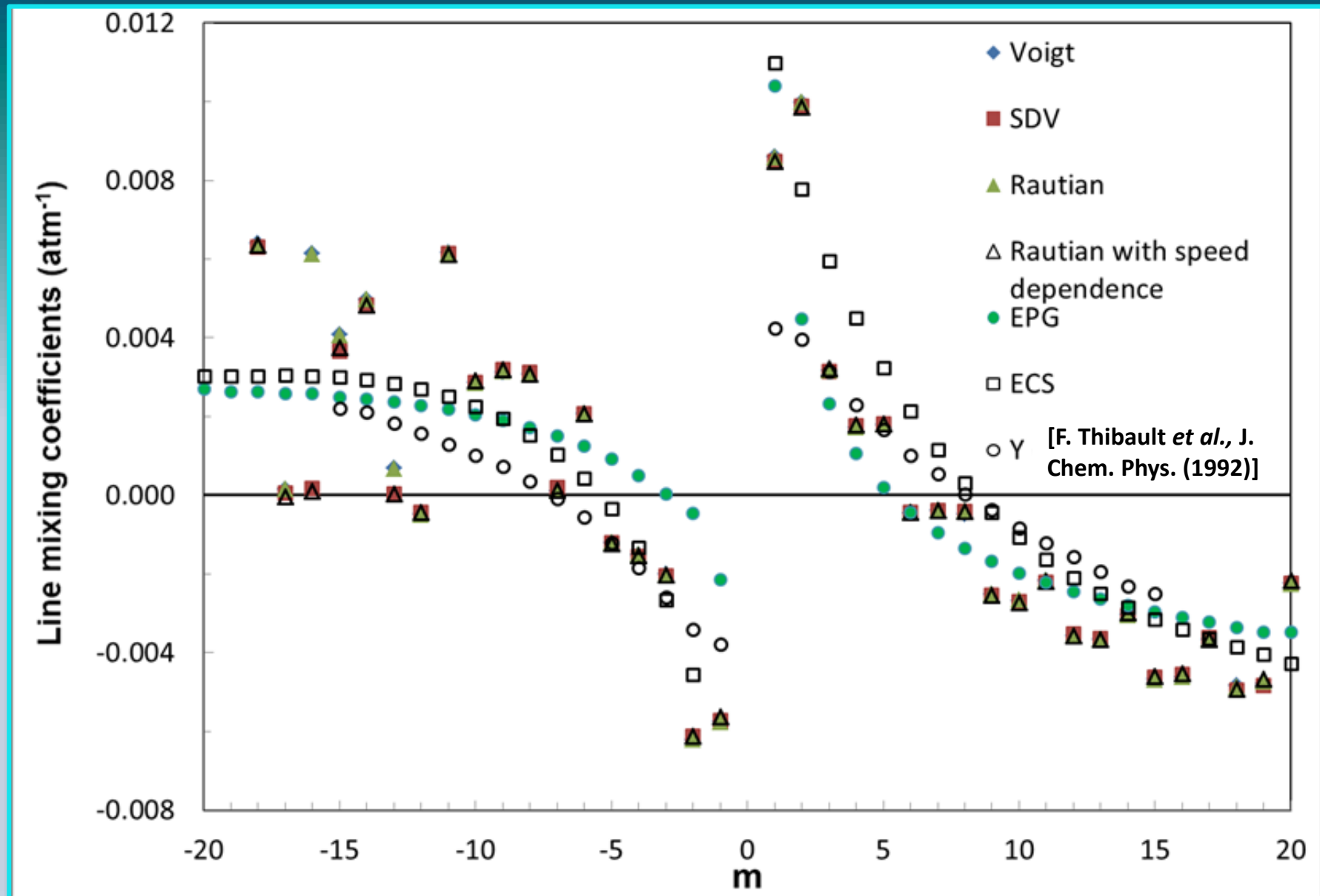
Line mixing coefficients determined using the Energy Corrected Sudden (ECS) Approximation



Optimized values of ECS parameters for the CO-Air system

<i>Parameters</i>	$A(\text{cm}^{-1}\text{atm}^{-1})$	λ	$d_c (\text{cm})$	β
<i>Values</i>	0.00315	0.55	3.8	0.065

Measured, calculated and previously published CO-He collisional line mixing coefficients (in $\text{cm}^{-1} \text{atm}^{-1}$ at 296 K) for transitions in the $1 \leftarrow 0$ band of CO.



Conclusions

- We have studied CO-CO, CO-air and CO-He spectra using a unconstrained multispectrum approach.
- The self- and foreign-broadened line parameters have been retrieved using the Voigt, speed dependent Voigt, Rautian, and Rautian with speed-dependence line shape models. Temperature dependences of pressure induced air-broadening and shift coefficients at different temperature were retrieved.
- The best agreement was found for the speed dependent models when line mixing is accounted for.
- We have used theoretical calculations using a potential energy surface to compute the He-narrowing parameters at different temperatures, the He-broadening and He-induced pressure shift coefficients and compare them with our experimentally determined parameters and with previously published results.
- Our retrieved He-broadening coefficients were found to agree very well with the corresponding close coupled calculated values at different temperatures.
- We present the first results of calculations of self-broadened width coefficients of CO using classical impact theory. We have used a simple interaction PES, with good results for half-widths of the molecular system.
- The diffusion constants for CO-CO and CO-He mixtures were determined using molecular dynamics calculations.
- The weak line mixing coefficients have been compared with results of semi-empirical calculations using the Exponential Power Gap law, the Energy Corrected Sudden approximation, and also with published results obtained from quantum dynamical calculations and were found to be in satisfactory agreement.

Future directions for research

- Conduct retrievals of line parameters using the Hartmann-Tra model recommended by IUPAC using the results of this study for parameters where there were no prior experimental or theoretical data
- Further investigate the behavior of line parameters at cryogenic temperatures
- Record new spectra for pure CO to enable the analysis of a wider range of lines.

References

1. L. Galatry, Simultaneous Effect of Doppler and Foreign Gas Broadening on spectral Lines
Physical Review **122**, 1218 (1961).
2. S.G. Rautian, I.I. Sobelman, Effect of Collisions on Doppler Broadening of Spectral Lines.
Soviet Physics Uspekhi-Ussr **9**, 701-& (1967).
3. Smith, B.C., Fundamentals of Fourier Transform Infrared Spectroscopy 1996, Boca Raton: CRC Press.
4. Egevs kaya, T.B., A Small Interferometer-a Double Cat's Eye-for Rapid-Scanning Fts. Infrared Physics, 1984. **24(2)**:
p. 329-331.
5. Mantz, A.W., V. Malathy Devi, D. Chris Benner, M.A.H. Smith, A. Predoi-Cross, and M.
Dulick, A Multispectrum Analysis of Widths and Shifts in the 2010–2260 cm⁻¹ Region of
12C16O Broadened by Helium at Temperatures between 80 and 297 K. Journal of Molecular
Structure, 2005. **742(1–3)**: p. 99-110.
6. D. C. Benner, C. P. Rinsland, V. Malathy Devi, M. A. H. Smith, and D. Atkins, "A multispectrum nonlinear least
squares fitting technique," J. Quant. Spectrosc. Radiat. Transfer 53, 705-721 (1995).
7. A. Levy, N. Lacombe, C. Chackerian, in:, K. Narahari Rao, Spectroscopy of the Earth's Atmosphere and of the
Interstellar Medium.
8. J.-M. Hartmann, C. Boulet, D. Robert, Collisional Effects on Molecular Spectra.Elsevier, 2008. Academic Press,
New York, 1992.
9. Zou, Q. and P. Varanasi, New Laboratory Data on the Spectral Line Parameters in the 1-0 and 2-0 Bands of ³⁷
12C16O Relevant to Atmospheric Remote Sensing. Journal of Quantitative Spectroscopy and Radiative Transfer, **2002**,
2002. **75(1)**: p. 63-92



Acknowledgements

The research carried out at the University of Lethbridge is funded by the Natural Sciences and Engineering Research Council of Canada through the Discovery and CREATE grant programs. The part of the research carried out at the College of William and Mary, Connecticut College and NASA Langley Research Center have been funded by cooperative agreements and contracts with the National Aeronautics and Space Administration. We thank Nazrul Islam, Koorosh Esteki and Hoimonti Rozario for their contributions to this project. Dr. D. Chris Benner at the College of William and Mary is thanked for allowing us to use his multispectrum fitting software in analysing the data.

Thank you!



“Man must rise above the atmosphere and beyond to fully understand the world in which he lives”, Socrates

University of
Lethbridge



Alberta Terrestrial Imaging Centre

AMETHYST



NSERC
CRSNG



TECTERRA



Natural Resources
Canada

Ressources naturelles
Canada